Taylor & Francis
Taylor & Francis Group

RESEARCH ARTICLE

  OPEN ACCESS   Check for updates
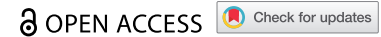
Induction of tissue resident memory T cells by measles vaccine vector

Heidy Vera-Peralta[a,b], Claude Ruffié[a], Valérie Najburg[a], Matthias Brione[b], Chantal Combredet[a], Phanramphoei Frantz[a], Jean-Nicolas Tournier[c], Frédéric Tangy[a], and Marie Mura [b]

[a]Institut Pasteur-Oncovita Joint Laboratory, Université Paris Cité, Institut Pasteur, Paris, France; [b]Interactions hôte-pathogène, Institut de Recherche Biomédicale des Armées, Brétigny-sur-Orge, France; [c]Division recherche et innovation, Académie du Service de santé des armées, Paris, France

ABSTRACT

Measles live attenuated vaccine (MV) induces strong humoral and cellular systemic memory responses allowing the successful control of measles since decades. MV has also been adapted into a promising vaccine platform with several vaccine candidates in clinical development. To understand and document the tissue-scaled memory response induced by MV, we explored the specific induction and persistence of resident memory T cells (Trm) in the lungs and the liver, two critical targeted tissues for vaccine development against several diseases. Trm are a subset of non-circulating highly specialized T cells. They are found at multiple barrier and mucosal sites, conveniently positioned to rapidly react against pathogens. The induction of Trm in different tissues is therefore critical for vaccine development. We demonstrated in mice the rapid generation of MV-specific and vectorized antigen-specific Trm in the liver and the lungs after a single dose, whatever the route of immunization. The intranasal route induced more Trm in the lungs than other routes, confirming the potential of intranasal vaccine administration of replicative viral vectors to generate a strong pulmonary immune response. MV-specific Trm cells were functionally active, with CD8$^+$ Trm secreting granzyme B upon in vitro restimulation and CD4$^+$ Trm cells secreting IFN-γ and TNF-α. We confirmed in human lymphocytes this tissue tropism by showing an overexpression of homing receptors directing them to epithelial and inflamed tissues. Vaccination strategies able to induce Trm cells at key sites represent a promising field to improve current vaccines, prioritize vaccine platforms and design future vaccines with enhanced protective efficacy.

Introduction

Live attenuated measles vaccine (MV) is one of the safest and most effective human vaccines. It has protected billions of children against this highly contagious acute respiratory illness since its introduction as global mass vaccination, reducing considerably childhood mortality.[1,2]

Measles virus is an enveloped, non-segmented single-stranded RNA virus, belonging to the Morbillivirus genus of the *Paramyxoviridae* family. The different vaccine strains were derived from the wild type Edmonston strain, empirically obtained by multiple passages in human and chicken embryo cells. Measles vaccine elicits strong humoral and cellular memory immune responses providing life-long immunity. Yet, the basis of measles virus attenuation and efficacy are not fully understood.[3] The elicited antibody and cellular immune responses mature over months.[4] Protection against the disease correlates with neutralizing antibody titers.[5–7] But cell-mediated immunity is essential for measles protection, as children with isolated agammaglobulinemia recover from measles[8] in contrast with individuals with T-cell deficiencies.[9–11] T cells are known to contribute indirectly to the protection by their collaboration with B cells and the clearance of viral RNA.[12] Circulating memory CD4$^+$ and CD8$^+$ T cells are detected years after measles immunization,[13]

but with different dynamics, the CD8$^+$ response being more sustainable over time.[14]

Little is known about the induction of tissue immunity by measles vaccine. Particularly, Trm cells are a highly specialized T cell population that once differentiated remains into the tissues.[15] They are transcriptionally, phenotypically, and functionally distinct from circulating central and effector memory populations.[16] Common features of Trm subset in different tissues are the downregulation of egress markers like S1PR1 and CCR7 and the upregulation of CD69 molecule. CD69 is considered as an early activation marker[17] but in the absence of an ongoing infection, its presence is a hallmark of tissue residency.[18] Trm cells upregulate integrins that promote tissue retention by interacting with their corresponding ligands on tissue surface. Depending on tissue location, Trm cells express different homing tissue markers adapted to their microenvironment (e.g., CD103 and CD49a molecules on epithelial and lung Trm cells or CD11a on liver Trm cells).[19–21] These cells are found in multiple tissues like the skin, lungs, liver, brain, genital mucosa, and gastrointestinal tract.[22] Due to their privileged location at pathogen entry sites, they act as a first defense line before the recruitment of antigen-specific cells from the circulating blood. CD8$^+$ Trm are well described for

---

several pathogens. They can release cytotoxic molecules as granzyme B and perforins, as well as IFN-γ and other chemokines activating innate immune effectors and promoting the recruitment of other cellular types to the infection site.[23,24] CD4^{+} Trm are less well described but there is now evidence that they play a central role in tissue protective immunity, especially in mucosal sites.[25,26] The memory response in human tissues is hardly assessable. Nevertheless, it is possible to measure the specific induction of tissue homing markers at the surface of circulating T cells to map the pattern of migration of the immune response.[27–30]

The induction of Trm cells by vaccines is a new field of intense research. Indeed, several studies in mouse and humans showed that their induction was associated with protection against respiratory infections.[31–37] Other tissues than the lungs are also targets of interest for the induction of Trm cells by vaccines. The immune response in the liver, for instance, is critical for malaria protection[38] or to fight hepatotropic viruses like hepatitis B[39] and hepatitis C viruses.[40] Also, the skin, the brain, and the mucosal barriers (gastrointestinal tracts, upper respiratory airways, genital mucosa) are of great interest. The COVID-19 pandemic revolutionized the field of vaccinology and revealed a huge quantity of vaccine platforms that are available for vaccine development. Therefore, it is important to document the quality, the quantity, the location, and the duration of the immune responses induced by each technology to be able in the future to prioritize the vaccine development regarding the required immune response for a defined pathogen.

Measles vaccine has been adapted as a replicative viral vector to deliver foreign antigens for more than 20 years.[41] The very immunogenic and attenuated Schwarz strain offers the possibility to add foreign gene sequences up to 7 kb in length in MV genome.[41] Importantly, the measles preexisting immunity has no negative impact on the vector immunogenicity against another pathogen.[42,43] This highly versatile platform was used to develop a variety of MV-based vaccine candidates against different pathogens. The MV-Chikungunya vaccine was particularly successful in phase 2 clinical trial, and other MV-vaccine candidates are in the clinical trial pipeline.[43–46] We hypothesized that this replicative viral vector could induce a local memory immune response in several tissues that would be useful to target pathogens with a specific tissue or mucosal tropism.

The objective of this work was to explore the specific induction of Trm by measles vaccine in a mouse model. We aimed at better understanding measles vaccine efficacy and providing data on the broaden immune responses generated by measles vaccine platform. We describe the generation of MV-specific Trm cells in the liver and the lungs 21 days after a single immunization with MV Schwarz by different immunization routes. Noteworthy, intranasal vaccination induced a higher proportion of Trm cells in the lungs, whereas the route of immunization did not modify the Trm response in the liver. MV specific CD8^{+} and CD4^{+} Trm were functionally active, secreting respectively Granzyme B and TNF-α/IFN-γ. We further used recombinant MV-malaria[47] and MV-SARS-CoV-2[48] vaccine candidates as models to confirm the induction of specific Trm against vectorized antigens. Finally, we expanded our results to human primary cells by demonstrating that measles-stimulated lymphocytes significantly over-express homing receptors that direct them to epithelial and inflamed tissues.

Results

Resident memory T cells are induced in lungs and liver after a single intraperitoneal administration of measles Schwarz vaccine

To study the ability of MV Schwarz vaccine to induce MV-specific tissue resident memory (Trm) CD8^{+} T cell responses, two groups of 6–10 weeks old hCD46^{+}/IFNAR^{−/−} mice were immunized intraperitoneally (IP) with a single administration of 10^5 TCID$_{50}$ of MV Schwarz virus or mock-injected (opti-MEM medium). Twenty-one days post immunization, the livers, spleens, and lungs were collected, and lymphocytes were extracted from the tissues. The surface staining of specific clusters of differentiation and the use of an MV-dextramer (DextrMV, H$_{22−30}$) allowed differentiating five populations in the liver: (i) CD8^{+} T cells (CD3^{+} CD8^{+}); (ii) CD8^{+} Trm (CD3^{+} CD8^{+} CD69^{+} CD62L^{−} CD11a^{+} KLRG1^{−} CXCR3^{+} CXCR6^{+}); (iii) MV-specific CD8^{+} Trm (CD3^{+} CD45RA^{−} CD8^{+} CD69^{+} CD62L^{−} CD11a^{+} KLRG1^{−} CXCR3^{+} CXCR6^{+} DextrMV^{+}); (iv) CD3^{+}CD8^{−} T cells; (v) CD3^{+}CD8^{−} Trm (CD3^{+} CD8^{−} CD69^{+} CD62L^{−} CD11a^{+} KLRG1^{−} CXCR3^{+} CXCR6^{+}). We also distinguished five populations in the lungs: (i) CD8^{+} T cells (CD3^{+} CD8^{+}); (ii) CD4^{+} T cells (CD3^{+} CD4^{+}); (iii) CD4^{+} Trm (CD3^{+} CD4^{+} CD44^{+} CD62L^{−} CD69^{+} CXCR3^{+} CD49^{+}); (iv) CD8^{+} Trm (CD3^{+} CD8^{+} CD44^{+} CD62L^{−} CD69^{+} CXCR3^{+} CD49^{+}); (v) MV-specific CD8^{+} Trm (CD3^{+} CD8^{+} CD44^{+} CD62L^{−} CD69^{+} CXCR3^{+} CD49^{+} DextrMV^{+}).

The liver CD8^{+} T cell population was similar in the immunized and control group, as well as the total CD8^{+} Trm cell population (Figure 1a). MV-specific CD8^{+} Trm were found in the liver in the immunized group ($p < 0.001$ for percentage, and absolute number of MV-specific CD8^{+} Trm cells). Regarding the CD4^{+} T cell population, the percentage of total CD3^{+}CD8^{−} Trm was higher in MV-immunized group compared to control group ($p = 0.0304$). There was no specific dextramer-staining in the panel to reveal the presence of MV-specific CD4^{+} Trm.

In the lungs (Figure 1b), we observed a significantly higher relative percentage and absolute number of CD8^{+} Trm cells ($p = 0.0022$ for both parameters) in immunized mice compared to control mice. As expected, only immunized mice had MV-specific CD8^{+} Trm in the lungs ($p = 0.0022$ and $p = 0.0049$ for percentage and absolute number of MV-specific CD8^{+} Trm cells). Lung CD4^{+} Trm population was higher in MV-immunized group compared to control group regarding the relative percentage ($p = 0.0247$) or the absolute number ($p = 0.0151$) of CD4^{+} Trm cells.

For the liver and the lungs, we identified Trm populations by using homing receptor markers expressed predominantly by liver Trm (CXCR6 and CXCR3) and lung Trm (CD49a and CD103), and we confirmed the specificity of dextramer staining by comparing dextramer[+] H$_{22−30}$ cells on control and MV Schwarz immunized group (Figure 1c–e).
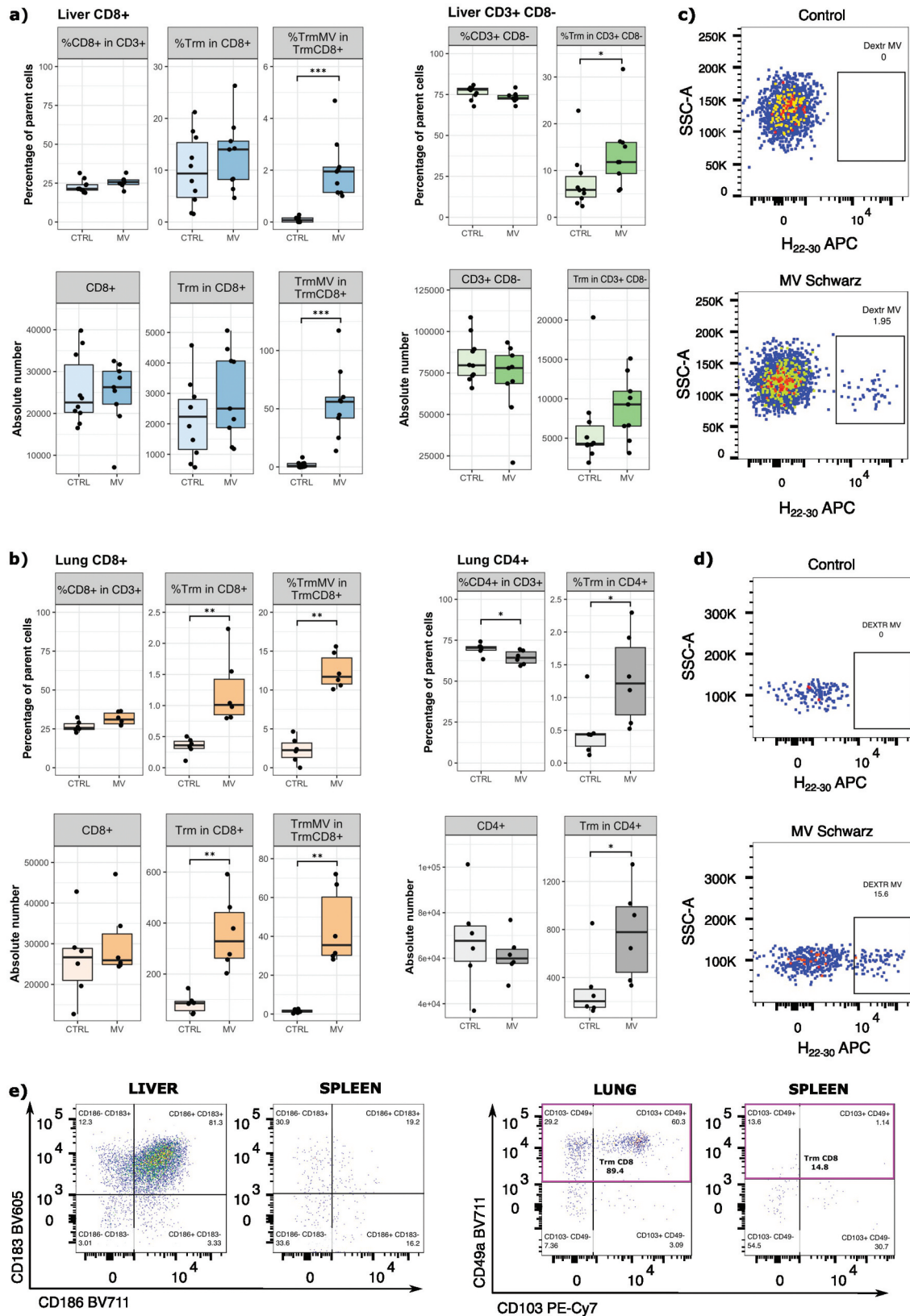
Figure 1. Induction of tissue resident memory T cells in mice after a single MV Schwarz immunization. hCD46$^+$/IFNAR$^{-/-}$ mice (n = 4–6 per group) were immunized by IP route with 10^5 TCID$_{50}$ of MV Schwarz or were mock-injected (opti-MEM mediumMEM). Twenty-one days post-immunization, lymphocytes were extracted from organs (liver, lungs, and spleen) and surface markers were stained to identify the different subpopulations. (a) Percentage and absolute number of CD8$^+$ T cells, resident memory CD8$^+$ T cells (CD8$^+$ Trm), measles-specific Trm (TrmMV), CD3$^+$CD8$^-$ T cells, and resident memory CD3$^+$CD8$^-$ T cells in the liver. (b) Percentage and absolute number of CD8$^+$ T cells, resident memory CD8$^+$ T cells (CD8$^+$ Trm), measles-specific trm (TrmMV), CD4$^+$ T cells, and resident memory CD4$^+$ T cells (CD4$^+$ Trm in the lungs. (c) Representative flow cytometry plots demonstrating the detection of liver mv-specific dextramer H$_{22-30}$ (gated on CD8$^+$ CD69$^+$ KLRG1$^-$ CD62L$^-$ CD11a$^+$ CXCR6$^+$ CXCR3$^+$) on control or MV Schwarz immunized mice. (d) Representative flow cytometry plots demonstrating the detection of lung mv-specific dextramer H$_{22-30}$ (gated on CD8$^+$ CD44$^+$ CD62L$^-$ CD69$^+$ CXCR3$^+$ CD49$^+$) on control or MV Schwarz immunized mice. (e) Representative flow cytometry plots showing the specific lung and liver markers used to define tissue-resident T cell populations. Each data point represents an individual mouse. Data are compiled from two experiments and are represented as median with IQR (interquartile range). Significant differences between the groups were determined by the two-tailed Mann–Whitney test (*p < .05, **p < .01, ***p < .001).

These data demonstrate the presence of MV-specific CD8^{+} Trm in the liver and the lungs after a single intraperitoneal injection of MV Schwarz vaccine strain and suggest the presence of MV-specific CD4^{+} Trm in both organs.

The induction of Trm in the liver is independent of the route of immunization, whereas the intranasal route induces higher Trm in the lungs

To evaluate the potential impact of the immunization route on the induction of CD8^{+} Trm in the liver, we immunized hCD46^{+}/IFNAR^{−/−} mice with 10^5 TCID$_{50}$ of MV Schwarz virus either intraperitoneally (IP), intravenously (IV), intramuscularly (IM), or intranasally (IN). We compared the percentage of CD8^{+} Trm in the tissue 21 days post-immunization.

In the liver (Figure 2a), the IM route induced the highest percentage of CD8^{+} T cells, followed by IP, IV and IN route. Although, the difference was statistically significant only between IM and IN route ($p = 0.0166$). The percentages of CD8^{+} Trm and MV-specific Trm were similar between all routes of immunization. All mice developed consistent systemic anti-MV responses as shown in Supplementary Table S1.

In the lungs (Figure 2b), the IV route generated a higher percentage of CD8^{+} T cells compared to the other immunization routes, but the difference was statistically significant ($p = 0.001$) only between IV and IN route. However, the proportion of CD8^{+} Trm cells was significantly increased after IN route compared to IM, IP, and IV immunization routes ($p = 0.0013$ for IN vs IM, $p = 0.0296$ for IN vs IP, and $p = 0.0106$ for IN vs IV). Likewise, the percentage of MV-
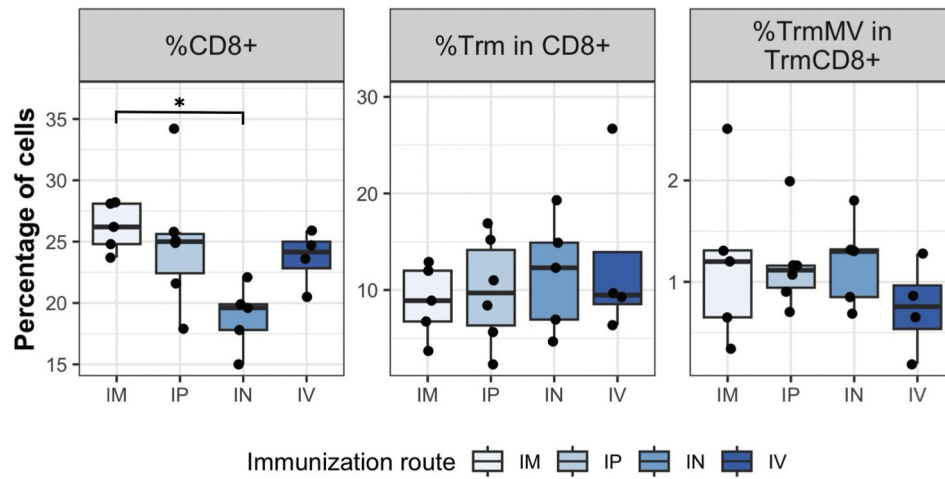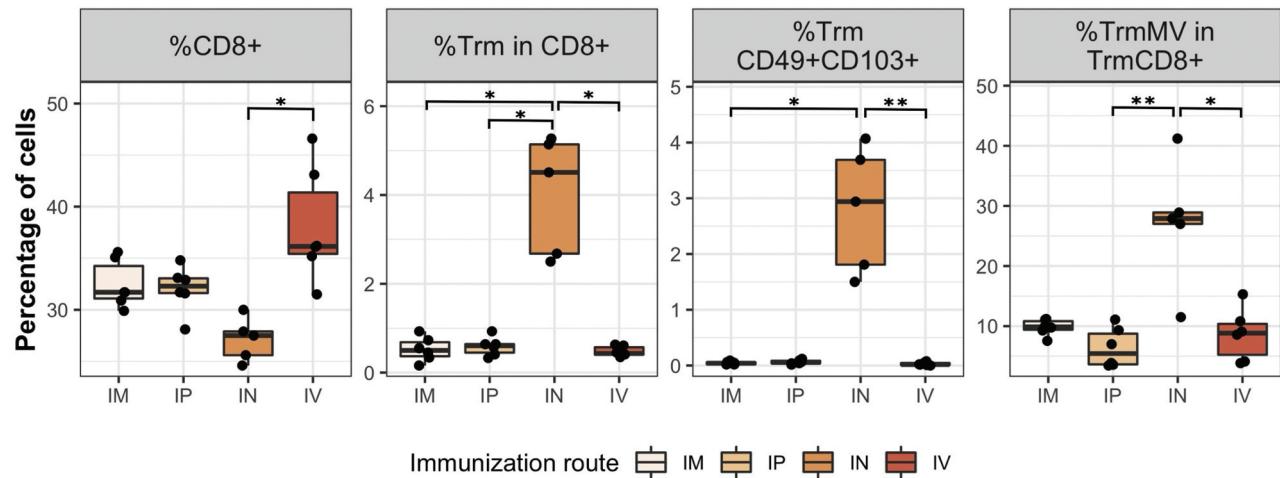
Figure 2. The immunization route differentially affects the induction of CD8^{+} Trm cells in the liver and the lungs. hCD46^{+}/IFNAR^{−/−} mice ($n = 4–6$ per group) were immunized by IM, IP, in or IV route with 10^5 TCID$_{50}$ of MV Schwarz. Twenty-one days post-immunization, lymphocytes were extracted from organs (liver, lungs, and spleen). (a) The percentage of CD8^{+} T cells (CD8^{+}), resident memory CD8^{+} T cells (CD8^{+} Trm) and measles specific Trm (TrmMV) were determined in the liver of immunized animals. (b) The percentage of CD8^{+}, CD8^{+} Trm, Trm CD49^{+} CD103^{+}, and TrmMV were determined in the lungs of immunized animals. Each data point represents an individual mouse. Data are compiled from one independent experiment. Data are represented as median with IQR. Significant differences between the groups were determined by the non-parametric Kruskal–Wallis test. Pairwise comparisons between groups were calculated using Dunn test and p-values were adjusted applying the Benjamini-Hochberg correction. (*$p < .05$, **$p < .01$).

specific Trm was higher in IN group compared to the other groups (p = 0.0032 for IN vs IP, p = 0.0201 for IN vs IV). Interestingly, IN vaccination route generated the highest percentage of double positive CD49a$^+$ and CD103$^+$ CD8$^+$ Trm cells (*p = 0.0032* for IN vs IM, and *p = 0.0201* for IN vs IV).

Overall, these results indicate that all immunization routes were equally able to generate MV-specific CD8$^+$ Trm in the liver. Nevertheless, the IN route was better at inducing MV-specific CD8$^+$ Trm in the lungs, despite the generation of a higher CD8$^+$ T cell response by IV route.

Measles-specific CD8$^+$ Trm cells have cytotoxic properties, and CD4$^+$ Trm secrete TNF-α and/or IFN-γ

To evaluate the functionality of induced CD8$^+$ and CD4$^+$ Trm cells, two groups of 6–10 weeks old hCD46$^+$/IFNAR$^{-/-}$ mice were immunized intranasally (IN) with a single administration of 10^5 TCID$_{50}$ of MV Schwarz virus or mock-injected (opti-MEM medium). We focused on the lungs after IN route of immunization to get the higher number of Trm necessary for functional studies. Twenty-one days post immunization, the lungs were collected, and lymphocytes were extracted from the tissues and stimulated *ex-vivo* with MV Schwarz virus at MOI = 1, PMA/Ionomycin or with media only. After MV Schwarz stimulation, the absolute number of total CD8$^+$ Trm cells (Figure 3a) and MV-specific CD8$^+$ Trm cells (Figure 3b) was significantly higher in MV-immunized group compared to control group (*p = 0.0095* and *p = 0.013*). MV-specific CD8$^+$ Trm cells secreted mainly Granzyme B (Figure 3c) and a lower proportion of cells were polyfunctional and secreted also TNF-α and/or IFN-γ (Figure 3d). However, due to the low number of cells producing IFN-γ and TNF-α, this polyfunctional attribute should be interpreted with caution. Likewise, total CD8$^+$ Trm also secreted Granzyme B as main cytokine and only a small portion secreted TNF-α or IFN-γ (Supplementary Figure S1).

Regarding CD4$^+$ T cells population, there was no significant difference in the absolute number of activated CD4$^+$ CD69$^+$ T cells between immunized and control group. However, the absolute number of cells expressing at least one cytokine was significantly higher (*p = 0.0095*) in MV Schwarz immunized group compared to control group (Figure 4a). Moreover, CD4$^+$ CD69$^+$ T cells secreted TNF-α, IFN-γ or both cytokines at the same time (Figure 4b).

These results confirm the cytotoxic potential of generated MV-specific CD8$^+$ Trm cells and the immune activating potential of CD4$^+$ CD69$^+$ T cells in mice immunized with MV Schwarz strain.

Measles-specific CD8$^+$ Trm cells declines over time but are maintained until 90 days post-immunization

To evaluate the longevity of tissue resident immune responses and if the route of immunization has an impact on the induction of functional tissue responses, two groups of 6–10 weeks old hCD46$^+$/IFNAR$^{-/-}$ mice were immunized intranasally (IN) or intramuscularly (IM) with a single administration of 10^5 TCID$_{50}$ of MV Schwarz virus. Ninety days post

immunization, the lungs were collected, and lymphocytes were extracted from the tissues and stimulated *ex-vivo* with MV Schwarz virus at MOI = 1, PMA/Ionomycin or with media only.

MV-specific Trm cells were still found in the lungs after both routes of administration (Figure 5a). However, the absolute number was small as compared to the one obtained at Day 21. After MV Schwarz stimulation, the absolute number of CD8$^+$ Trm cells producing GrzB was significantly higher in IN immunized mice (*p = 0.01*) compared to IM immunized group. There was no difference in TNF-α or IFN-γ-producing cells (Figure 5b). CD8$^+$ Trm cells secreted mainly Granzyme B in IN-immunized mice while IM-immunized mice secreted mostly TNF-α (Figure 5c).

Regarding CD4$^+$ T cells population, there was no significant difference in the absolute number of CD4$^+$ CD69$^+$ T cells expressing IFN-γ- or TNF-α in IM compared to IN immunized group (Figure 5d). In IN-immunized mice, CD4$^+$ CD69$^+$ T cells secreted mostly TNF-α and in IM-immunized mice either TNF-α or a combination of TNF-α and IFN-γ (Figure 5e).

Thus, we confirm the maintenance of MV-specific Trm in the lungs ninety days after a single immunization, even though the absolute numbers markedly decline over the time.

Immunization with recombinant MV generates Trm against the vectorized antigens

Next, we assessed if the MV vector platform was able to induce Trm against vectorized antigens. Trm in the liver are essential to control malaria and so we used a recombinant MV expressing a *Plasmodium berghei* fusion antigen (MV-Pbfusion) to evaluate the induction of Trm by MV vector in the liver. Pbfusion is composed of four different Pb antigens containing CD8$^+$ T cell epitopes.[49] Two groups of hCD46$^+$/IFNAR$^{-/-}$ mice were immunized IP with 10^5 TCID$_{50}$ of MV-Pbfusion or were mock-injected (opti-MEM medium). The livers were collected twenty-one days post immunization to evaluate the memory CD8$^+$ T cell responses. As shown in Figure 6a,b, the immunization with MV-Pbfusion generated both MV-specific and Pbfusion-specific Trm in the liver as compared to the control group (*p < 0.001 for both*). To assess the presence of CD8$^+$ Trm in the lungs, we used a recently developed measles SARS-CoV-2 vaccine candidate expressing a stable form of the Spike protein (MV-SARS-CoV-2) that protects mice and golden Syrian hamsters from intranasal SARS-CoV-2 infectious challenge.[48] Two groups of hCD46$^+$/IFNAR$^{-/-}$ mice were immunized IN with 10^5 TCID$_{50}$ of MV-SARS-CoV-2 or were mock-injected (opti-MEM medium). We observed a significantly higher number of MV-specific Trm (*p = 0.0128*) and SARS-CoV-2-specific Trm (*p = 0.0095*) in MV-SARS-CoV-2 immunized mice as compared to the control group (Figure 6c,d).

Together these results demonstrate the ability of MV vaccine platform to induce the generation of CD8$^+$ Trm cells specific to the vector itself and to an expressed antigen in two different tissues, the liver and the lungs.
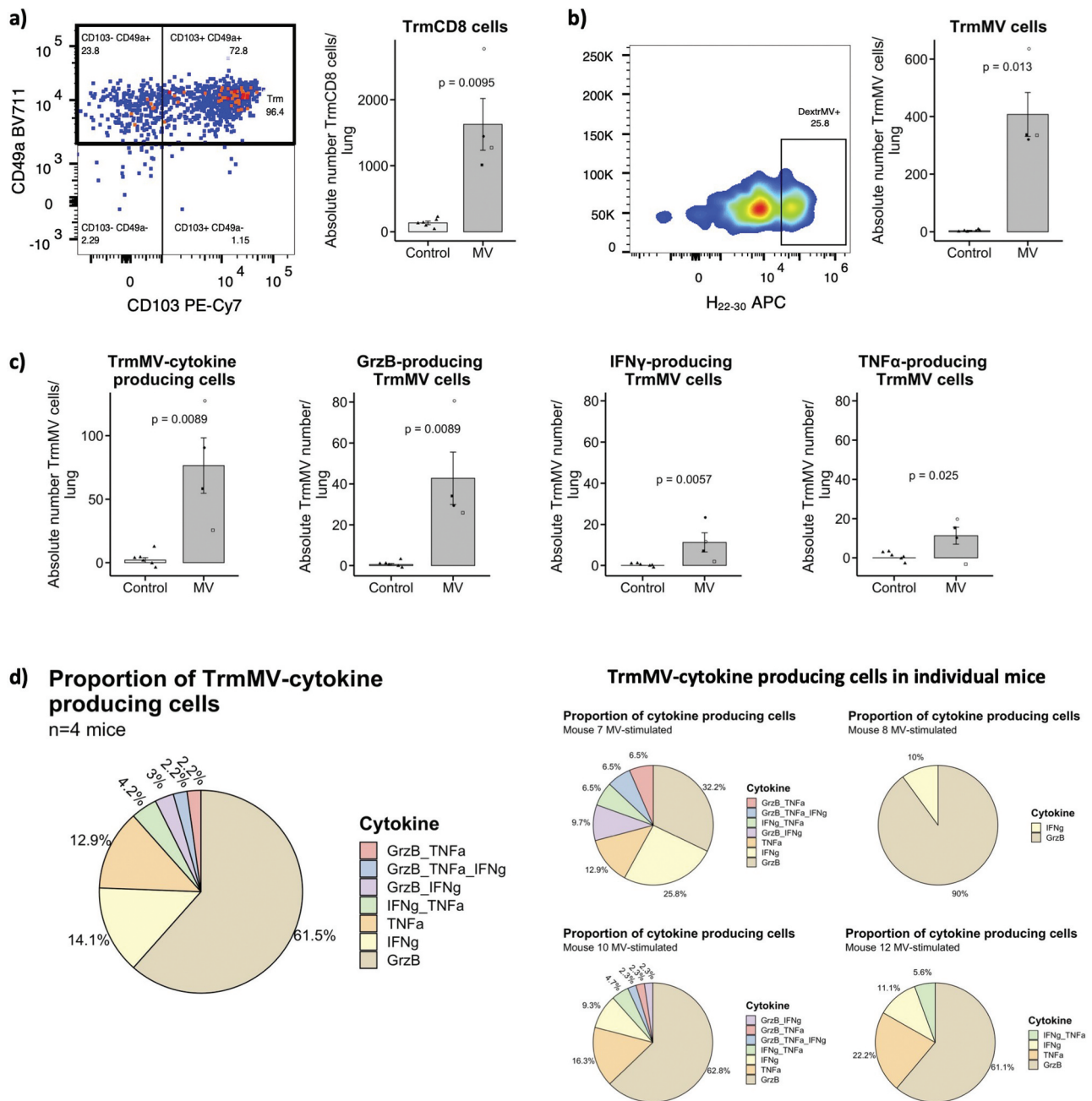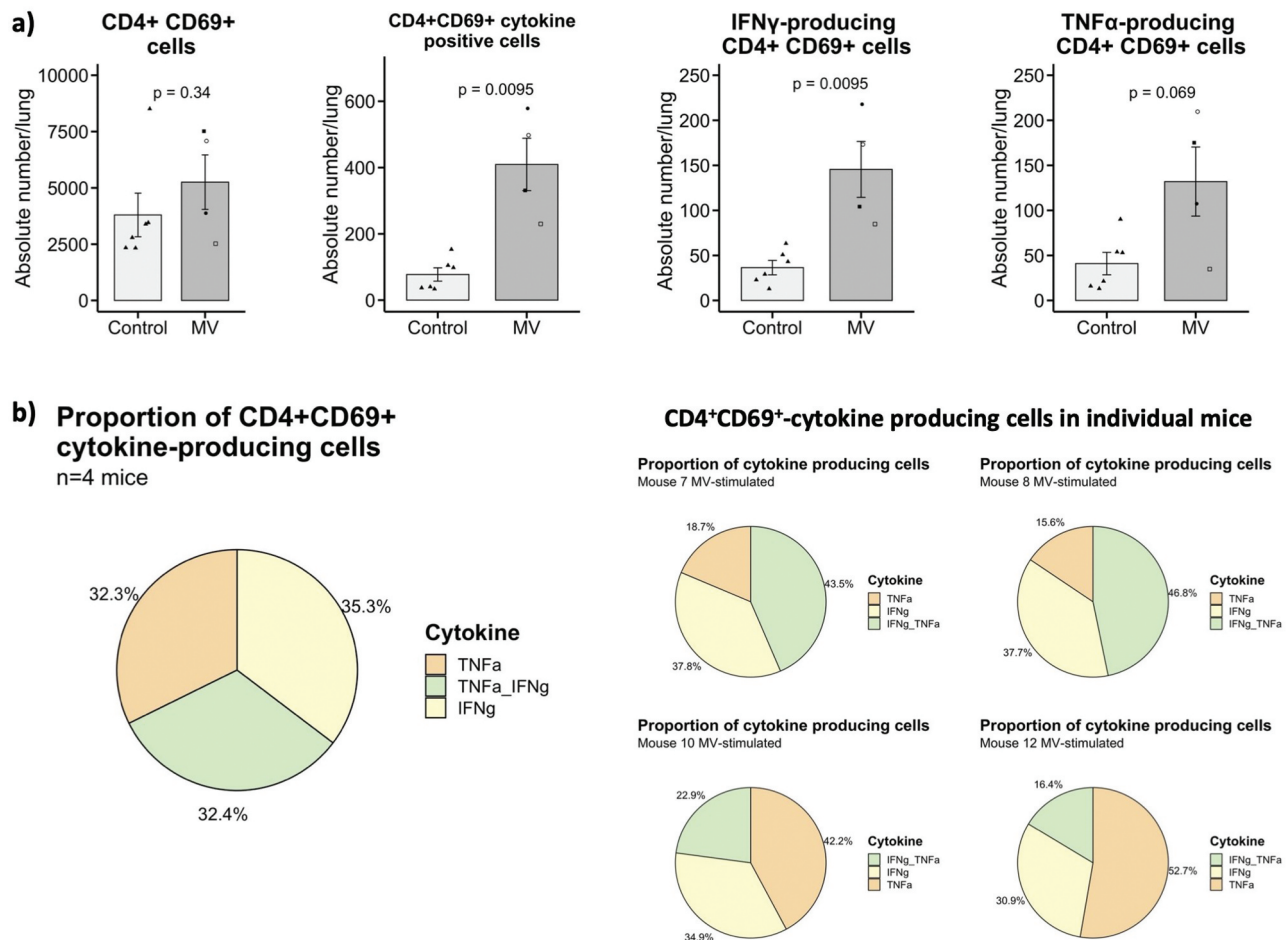
Figure 3. Cytokine expression profile of CD8^{+} Trm cells. (a) Representative flow plots and graphs showing the CD8^{+} Trm population (gated on CD8^{+} CD44^{+} CD62L^{−} CD69^{+} CXCR3^{+}) and the absolute number of CD8^{+} Trm cells/lung in MV Schwarz versus control group. (b) Representative flow plots and graphs showing the MV-specific CD8^{+} Trm population (gated on CD8^{+} CD44^{+} CD62L^{−} CD69^{+} CXCR3^{+} CD49^{+} CD103[±]) and the absolute number of MV-specific Trm cells/lung in MV Schwarz versus control group. (c) Total count of TrmMV/lung producing at least one or more cytokines, total count of TrmMV/lung producing GrzB, IFN-γ or TNF-α. Each data point represents an individual mouse. Data are compiled from one independent ICS experiment at early time point (d21 post-immunization). Data are represented as mean with standard error. Significant differences between the groups were determined by the two-tailed Mann–Whitney test (*$p < .05$, **$p < .01$, ***$p < .001$). (d) Proportion of TrmMV producing only one cytokine or a combination of different cytokines in MV Schwarz immunized group (total and individual mice graphs).

Measles vaccine induces the overexpression of homing receptors in primary human T cells directing them into epithelial and inflamed tissues

As there is no identified specific marker of circulating pre-Trm in the blood in humans, we chose to study the expression of tissue-homing receptors at the surface of T cells. Indeed, these markers allow the recruitment and entry into the tissues, where the cells may be differentiated in Trm. We assessed the expression of ten different

homing receptors (Table 1) at the surface of activated CD4^{+} and CD8^{+} T cells after *in vitro* stimulation by UV-inactivated measles Schwarz virus or UV-inactivated SARS-CoV-2 Wuhan strain at a MOI of 1. We selected eight subjects with no previous history of COVID-19 infection or SARS-CoV-2 vaccination but being vaccinated by Measles-Rubella-Mumps (MMR) vaccine in childhood. The UV-inactivated SARS-CoV-2 stimulated samples served as a control of the expression of homing receptors

Figure 4. Cytokine expression profile of CD4+ cells. (a) Total count of CD4+ CD69+ T cells, CD4+ CD69+ T cells expressing at least one cytokine, CD4+ CD69+ T cells expressing IFN-γ or TNF-α per lung in MV Schwarz versus control group. Each data point represents an individual mouse. Data are compiled from one independent ICS experiment at early time point (d21 post-immunization). Data are represented as mean with standard error. Significant differences between the groups were determined by the two-tailed Mann–Whitney test (*p < .05, **p < .01, ***p < .001). (b) Proportion of CD4+ CD69+ T cells producing one cytokine or a combination of two cytokines in MV Schwarz immunized group (total and individual mice graphs).

in response to an inactivated virus stimulation *in vitro*, whereas the measles virus stimulation may engage the memory specific adaptive response. The unstimulated control represents the expression of homing markers by a small amount of preexisting activated CD69+ cells circulating at the time of blood collection. The overnight stimulation led to the upregulation of the activation marker CD69 that serves as a surrogate marker for antigen-specificity.[17] The comparison of the two stimulations revealed a higher number of MV-specific central memory CD8+ T cells expressing CCR9 and CD186 (Figure 7a), two chemokine receptors necessary for the entry into respectively the intestinal tract,[54] bone marrow,[63] inflamed tissues and the liver.[58] CD186 was also more expressed by MV-specific naïve CD8+ T cells and CD4+ T cells (Figure 6a,b). Lastly, CD103, a marker of epithelial homing into the intestine and the lungs was more frequently expressed by MV-specific naïve CD4+ T cells (Figure 7b). There was no significant differentially expressed homing receptor in effector memory T cells.

These results suggest that measles vaccine Schwarz virus induces in human a specific T cell tropism for epithelial and inflamed tissues.

Discussion

Vaccination strategies promoting protective immune responses at pathogen entry sites are highly desirable. In recent years, tissue resident memory T cells emerged as a key population involved in first line defense against pathogens previously encountered by the immune system or generated after vaccination.[64] One of the main advantages of the presence of Trm cells in the tissues is the possibility to neutralize pathogens at an early step of the infection cycle and, in some cases, even providing sterilizing immunity. In general, live attenuated viral vectors are good inducers of Trm cells compared to inactivated or subunits vaccines.[31] Their replicative property allows local and distant antigenic presentation to the immune system and the correct establishment of Trm responses.

The aim of this work was to explore the specific induction of Trm by live-attenuated measles vaccine (MV) or MV vector. We demonstrated in IFNAR−/− mice the generation of MV-
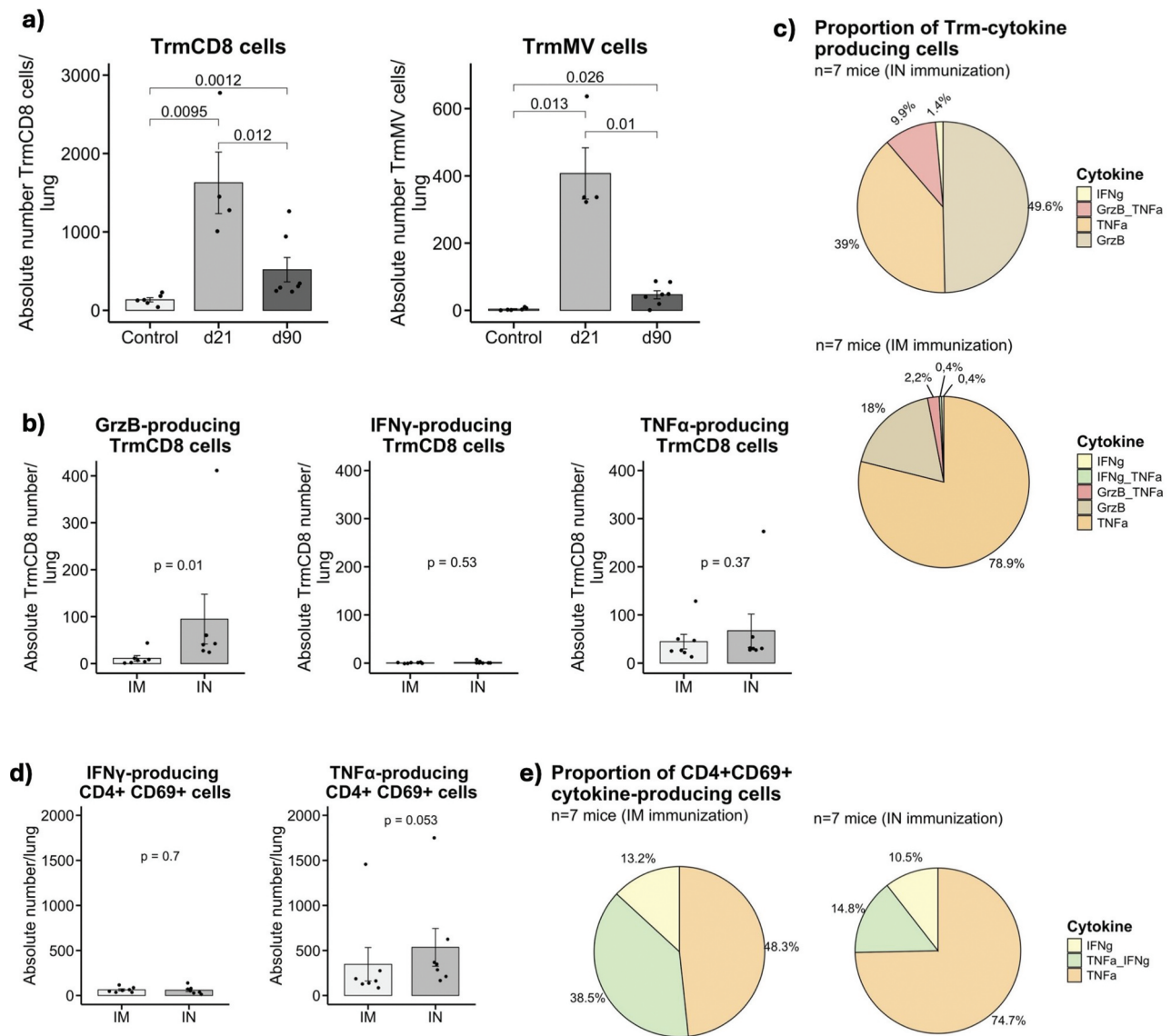
Figure 5. Longevity and functionality of Trm cells 90 days after a single immunization. (a) Absolute number of CD8+ Trm cells/lung and mv-specific CD8+ Trm cells/lung in immunized MV Schwarz group at 21 days p.l., 90 days p.l, or control group. (b) Total count of CD8+ Trm cells/lung producing GrzB, IFN-γ or TNF-α in IN versus IM MV Schwarz immunized group. (c) Proportion of CD8+ Trm producing only one cytokine or a combination of different cytokines in IN and IM MV Schwarz immunized group. (d) Total count of CD4+ CD69+ T cells/lung expressing IFN-γ or TNF-α in IN versus IM MV Schwarz immunized group. (e) Proportion of CD4+ CD69+ T cells producing one cytokine or a combination of two cytokines in IN and IM MV Schwarz immunized group. Each data point represents an individual mouse. Data at d21 in (a) are derived from the ICS experiment at early time point in Figure 3ab. Data at d90 (bcde) are derived from one independent ICS experiment at late time point. Data are represented as mean with standard error. Significant differences between the groups were determined by the two-tailed Mann–Whitney test (*$p < .05$, **$p < .01$, ***$p < .001$).

specific and vectorized antigen-specific Trm in the liver and the lungs after a single IP immunization with measles Schwarz vaccine or recombinant MV Schwarz vector. By using the dextramer technology, we confirmed the specificity of the response, though the number of real Trm is underestimated by focusing only on one specific epitope that captures around 2.5% of the systemic CD8+ T cell response. The use of an IFNAR$^{-/-}$ mouse model may also lower the magnitude of Trm induction. Indeed, mice lacking type-I IFN and MAVS signaling display impaired expansion of CD8+ Trm cells in the lungs and reduction in antigen specific production of granzyme B and IFN-γ.[65] Though this mouse model is necessary to study live-attenuated measles virus as type-I IFN is the species barrier and its presence does not allow viral replication.[66] MV-specific Trm were functionally active in this mouse

model, CD8+ Trm secreting granzyme B, and CD4+ Trm secreting IFN-γ and TNF-α upon *in vitro* restimulation. The predominant secretion of granzyme B by CD8+ Trm highlights their cytotoxic potential that may be recall for a fast viral clearance.[23] The rapid release of IFN-γ and TNF-α cytokines by CD4+ Trm[67] may lead to a fast recruitment of auxiliary immune cells to the infected site, potentiate CD8+ T cell response and enhance in the lungs the alveolar macrophages response.

We did not perform protection studies. Previous studies demonstrated the efficacy of MV-based vectors to generate protective immune responses against a variety of microorganisms at multiple tissue sites.[47,48,68] The specific involvement of Trm in protection is not easy to assess but several studies showed strong evidence of their major contribution to
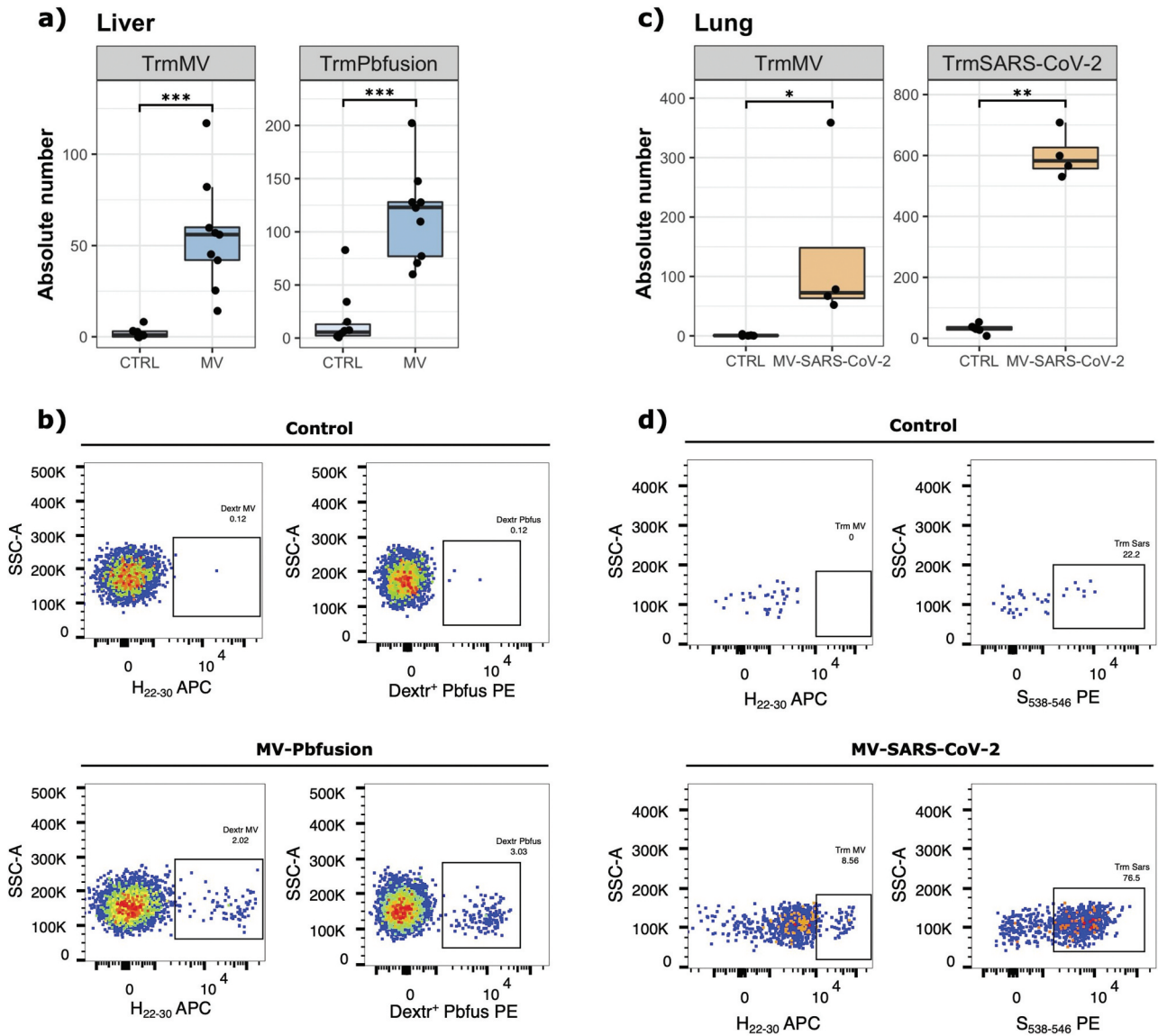
Figure 6. Generation of antigen specific Trm after immunization with MV viruses expressing vectorized antigens. (a) Absolute number of MV-specific and Pbfusion-specific CD8+ Trm cells in the liver of mice (n = 4–6 per group, two experiments) immunized IP with 10^5 TCID$_{50}$ of MV Pbfusion or mock-injected (opti-MEM medium), twenty-one days post immunization. (b) Representative flow cytometry plots demonstrating the detection of liver MV-specific and Pbfusion-specific dextramer (gated on CD8+ CD69+ KLRG1− CD62L− CD11a+ CXCR6+ CXCR3+) on control or MV Pbfusion immunized mice. (c) Absolute number of MV-specific and SARS-CoV-2-specific CD8+ Trm cells in the lungs of mice (n = 4–6 per group) immunized in with 10^5 TCID$_{50}$ of MV_SARS-CoV-2 or mock-injected (opti-MEM medium), twenty-one days post immunization. (d) Representative flow cytometry plots demonstrating the detection of lung MV-specific or SARS-CoV-2 specific dextramer (gated on CD8+ CD44+ CD62L− CD69+ CXCR3+ CD49+) on control or MV SARS-CoV-2 immunized mice. Each data point represents an individual mouse. Data are represented as median with IQR. Significant differences between the groups were determined by the two-tailed Mann–Whitney test (*p < .05, **p < .01, ***p < .001).

protection, and has been reviewed elsewhere,[69] also in the context of vaccine development.[70] Regarding measles infection, the neutralization titer defined the correlate of protection but the T cell response is essential[9–11] and Trm may play a role at the portal of entry. However, the goal of our study was rather to document the versatility of measles to induce Trm in different tissues for the future development of measles-vectorized vaccines against several pathogens.

The time requested for the generation of resident memory immune responses after immunization varies according to the model being studied but, in some cases, can be noted as soon as 7 days post immunization.[21,71–73] In the preliminary data obtained to prepare our study, a growing number of MV-specific CD8+ Trm cells were observed in the liver at 7,

14, and 21-days post-immunization after a single IP administration of MV Schwarz vaccine. There was no difference in the percentage of CD8+ Trm cells after a prime-boost immunization at one-month interval, compared to a single immunization. This may be explained by the fact that MV Schwarz vaccine disseminates evenly through mouse tissues and the administrated dose (10^5 TCID$_{50}$) generates a strong immune response, converting a second immunization dose unnecessary. Thus, for practical reason, we harvested organs at twenty-one days post immunization for this whole study. A key feature of Trm cells is their long maintenance in the tissues. However, this maintenance is dependent on multiple tissue-specific survival signals and not all Trm persist over the long term.[74] For instance, Trm localized in repair-associated memory depots

Table 1. List of homing receptor markers studied by flow cytometry on human stimulated T cells.

Marker	Receptor type	Ligand	Function	Marker-expressing cells	Reference
CD197 (CCR7)	Chemokine receptor	CCL19, CCL21	Entry into secondary lymphoid organs	Naïve T cells, memory T cell subsets	Brinkman 2013[50]
CCR10	Chemokine receptor	CCL27, CCL28	Entry into skin tissue	CD4+ T cells	Tubo 2011, Sigmundsdottir 2007[51,52]
CD185 (CXCR5)	Chemokine receptor	CXCL13	Entry into follicles of secondary lymphoid organs	Follicular helper T cells (Tfh), activated CD4 T cells	Chu 2019[53]
CDw199 (CCR9)	Chemokine receptor	CCL25	Entry into gut tissue, mucosal tissue	T cells	Mora 2003[54] Papadakis 2003[55]
CD194 (CCR4)	Chemokine receptor	CCL17	Entry into inflamed skin tissue	CD4+ T cells	Campbell 2007[56]
CD196 (CCR6)	Chemokine receptor	CCL20	Entry into inflamed epithelial tissue, gut tissue	Immature DC, Th17, Tcm and Tem, B cells, NKT cells	Ito 2011[57]
CD186 (CXCR6)	Chemokine receptor	CXCL16	Entry into inflamed tissues, liver, and lungs	T cells, NK cells, NKT cells	Tse 2014, Wein 2019[58,59]
CXCR3	Chemokine receptor	CXCL9, CXCL10, CXCL11	Entry into inflamed tissues	T cells, NK cells	Groom 2019[60]
CD103	Integrin	E-cadherin	Entry into epithelial tissues (lung, skin, human liver, gut)	T cells, DC	Mackay 2013, Thopam 2018[19,61]
CD161 (KLRB1)	C-type lectin	LLT1	Entry into inflamed tissue, enriched in T cells from gut and liver	CD4+ and CD8+ T cells, NK cells, NKT cells, monocytes, and dendritic cells	Konduri 2020[62]
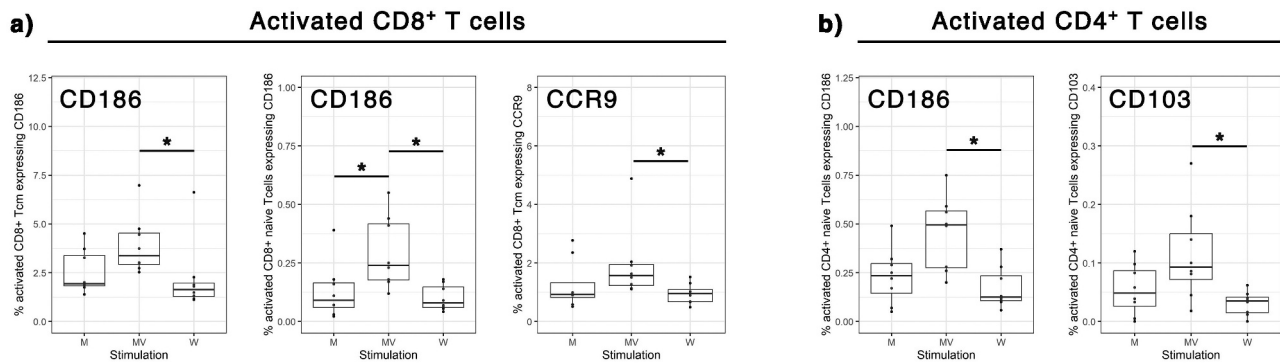
Figure 7. Expression of tissue homing receptors on MV-specific human T cells. Human PBMCs were unstimulated (M) or stimulated *in vitro* for 20h with UV-inactivated measles Schwarz strain (MV) or UV-inactivated SARS-CoV-2 Wuhan strain (W) at an MOI of 1. The expression of ten different tissue homing markers was assessed by flow cytometry. Cells were gated on antigen-specific T cells (CD69+ activated T cells). CD62L and CD45RO expressions were used to identify naïve T cells (CD62L$^+$ CD45RO$^-$), central memory T cells (Tcm, CD62L$^+$ CD45RO$^+$), effector memory T cells (Tem, CD62L$^-$ CD45RO$^+$) and terminally differentiated effector memory T cells (T$_{EMRA}$, CD62L$^-$ CD45RO$^-$). (a) Tissue homing receptors significantly over-expressed by measles-specific CD8$^+$ T cells subpopulations. (b) Tissue homing receptors significantly over-expressed by measles-specific CD4$^+$ T cells subpopulations. Each data point represents an individual human sample. Data are represented as median with IQR significant differences between the groups were determined by kruskal-wallis test, Dunn post-hoc test and a correction for multiple comparisons using the Benjamini–Hochberg correction (*$p < .05$ and fdr < 0.2).

(RAMD) are short-lived.[75] Live-attenuated measles virus induce long-term systemic immune memory responses and we hypothesized that MV-specific Trm are also maintained in the tissues for a long period of time. Indeed, we found MV-specific Trm in the lungs ninety days after a single immunization. However, the absolute number declined over the time. The waning of lung Trm cells has been described in other models of viral infection, such as influenza and RSV.[76,77] This may reflect an expected contraction of the response in the absence of local antigen stimulus,[78] possibly exacerbated by the absence of type-I IFN in the mouse model.[65] Indeed, previous toxicity studies found persistent viral RNA at 22 days in different tissues of hCD46$^+$/IFNAR$^{-/-}$ mice, especially lymphoid organs, that disappeared at day 90 post-immunization.[79] Also, memory T cells in the tissues may include multiple polyfunctional CD8 memory subsets,[80] including transient effector memory T cells, even though we used several specific markers to catch Trm only. Other

immune cell populations could participate to the maintenance of lung Trm cell responses. Alveolar macrophages were identified as source of local antigen in a model of vaccination with an adenovirus recombinant vector.[81] Another aspect to consider is the activation of the ARTC2.2/P2RX7 axis during cell isolation steps, which can induce Trm and NKT cell death through the formation of pores in the cellular membrane, thus affecting the outcome of subsequent functional studies.[82] All together, these factors may explain the observed loss of total and MV-specific CD8$^+$ Trm cells between days 21 and 90 post immunization.

An important consideration for CD8$^+$ T cells generation at the desired target site is the immunization route. Previous studies showed the relevance of liver CD8$^+$ Trm in the protection against malaria parasite in mice and non-human primates (NHP) models after immunization with radiation-attenuated sporozoites (RAS).[83–85] In both models, IV immunizations with RAS sporozoites were better inducers of liver functional

CD8^{+} T cell responses compared to IM or subcutaneous (SC) immunization route. Fernandez et al.[86] used a prime-and-trap strategy based on antigen delivery by dendritic cells (prime) followed by IV immunization with an adenovirus-associated virus vector for targeted-antigen expression on hepatocytes (trap). They demonstrated the generation of liver CD8^{+} Trm cells after IV immunization, which protected the immunized animals from an infectious challenge with PbANKA sporozoites. In contrast to these findings, IV immunization was not superior to other immunization routes using MV-malaria for liver CD8^{+} Trm induction. A possible explanation is that MV vector being replicative, it disseminates homogeneously into the tissues[66] and develops a significant number of Trm cells independently of the immunization route. Interestingly, IN immunization induced a higher number of lungs CD8^{+} Trm cells compared to IV, IM or IP routes. These results are consistent with data obtained in other studies using different viral vectors,[31,87–90] and recently with measles and mumps viral vectors delivering SARS-CoV-2 Spike protein.[68] This confirms the importance of the administration route to generate local memory responses for respiratory pathogens and brings into consideration the use of IN route to generate Trm at the respiratory tract. However, an important aspect to achieve is the appropriate delivery of antigens to the lower respiratory tract[91,92] to properly stimulate cellular adaptative immune responses in the lungs.

The study of human Trm responses is challenging due to the limited access to tissue samples. For lung Trm, a semi-invasive technique, the bronchoalveolar lavage fluid (BALF) can be used to study airway Trm.[92,93] For liver Trm, some studies were made in liver-transplanted patients showing that Trm cells can persist in the tissues even years after the transplant.[94,95] To bypass this difficulty, the study of homing receptors expressed by human PBMCs could be a useful tool.[30] A major part of measles memory T cells is located in the bone marrow[96] and the circulating counterpart may not fully reflect the immune landscape of measles vaccine-specific memory T cells. Still, previous studies succeeded at amplifying and stimulating memory T cells from whole blood years after measles-mumps-rubella vaccination.[13] In our study, we investigated the expression of ten surface markers on human PBMC samples after *in vitro* stimulation with UV-inactivated measles vaccine (live-attenuated measles vaccination in childhood) or UV-inactivated SARS-CoV-2 (unvaccinated individuals with no previous COVID-19, negative control). A higher expression of CXCR6 and CD103 markers were observed in MV-specific activated T cells, two core markers of Trm. CXCR6 plays a role in immunosurveillance through its interaction with CXCL16 that is expressed by epithelial cells.[97] It has also been described as an important marker for the recruitment of activated CD8^{+} in the liver.[98] Indeed, its ligand CXCL16 is constitutively expressed by liver sinusoidal endothelial cells.[99] Moreover, CXCR6 has been described as a homing marker of murine Trm in the bone marrow.[63] In humans, Trm of bone marrow preferentially maintain long-term memory for systemic pathogens like measles.[96] They are rapidly mobilized after antigen encounter to generate circulating memory T cells.[100] CD103 interacts with E-cadherin present on

epithelial cells, and supports tissue retention.[61] It has been associated with Trm in several tissues (skin, lung, brain, gut). Additionally, CCR9 marker was also highly expressed, indicating T cells with a mucosal phenotype.[55] These results are in accordance with our mouse findings, supporting the utility of homing markers as predictors of lymphocyte tissue migration patterns.

In summary, we demonstrated in mice the generation and persistence of functionally active resident memory CD8^{+} and CD4^{+} T cells in the lungs and the liver after a single immunization with live-attenuated measles vaccine or measles vector, whatever the route of immunization. Upon specific restimulation CD8^{+} Trm cells secreted Granzyme B and CD4^{+} Trm cells secreted IFN-γ and TNF-α. Confirming this tissue-tropism in human lymphocytes, measles vaccine induced an overexpression of homing receptors directing them to epithelial and inflamed tissues. Lastly, our results confirm the great versatility of live measles vaccine vector to generate strong immune responses against a variety of pathogens for which the induction of tissue memory responses is needed for protection.

Material and methods

Plasmid construction

The plasmid containing Pbfusion sequence was kindly provided by Dr. Rogerio Amino (Malaria Infection and Immunity Lab, Pasteur Institute). Pbfusion contained a malaria fusion protein expressing four different *Plasmodium berghei* antigens carrying CD8^{+} T cell epitopes. Primers introducing the restriction sites FseI and BssHII to the Pbfusion 5′ and 3′ ends, respectively, were used to amplify the nucleotides 1–2772 and were subsequently cloned into the pTM3-Schwarz plasmid. This plasmid coded for the antigenomic sequence of Schwarz measles vaccine strain and contained an additional transcription unit (ATU) to insert foreign genes between H and L genes. The complete sequence respected the "rule of six," stipulating that the number of nucleotides in the MV genome must be a multiple of 6. The plasmid sequence was verified by Sanger sequencing prior to rescue experiments.

Ethics statement

Cell lines

African green monkey kidney cells (Vero) and HEK293T7-NP helper cells (stably expressing MV-N and MV-P genes) were maintained at 37°C, 5% CO_2 in Dulbecco's modified Eagle medium (DMEM) (Thermo Fisher) supplemented with 5% or 10% heat-inactivated fetal bovine serum (FBS) (Corning) and 1% penicillin/streptomycin (Thermo Fisher).

Production and characterization of recombinant viruses

Recombinant viruses were produced by $CaCl_2$ transfection of HEK293T7-NP helper cells using the method described by Combredet et al.[41] Briefly, helper HEK293-T7-NP cells were transfected with 5 µg of pTM3 Pbfusion plasmid and 0.02 µg of pEMC-La expressing the MV polymerase L gene. After overnight incubation at 37°C, the transfection medium was replaced by fresh medium, and a heat shock was applied for 3 h at 42°C and then returned to 37°C. After two days of incubation at 37°C, transfected cells were transferred to 100-mm dishes with monolayers of Vero cells. Syncytia that appeared after 2–3 days of co-culture were singly picked and transferred onto Vero cells seeded in six-well plates. Infected cells were trypsinized and expanded in 75 cm^2 and then 150 cm^2 flasks, in DMEM with 5% FBS. To collect viruses, cells were scraped into a small volume of opti-MEM medium (Thermo Fisher), lysed by a single freeze-thaw cycle and cell lysates clarified by low-speed centrifugation. The infectious supernatant was then collected and stored at – 80°C. Titers of rMVs were determined on Vero cells seeded in 96-well plates infected with serial tenfold dilutions of virus in DMEM with 5% FBS. After incubation for 7 days, cells were stained with crystal violet, and $TCID_{50}$ values were calculated using the Karber method.[101] Virus growth kinetics of rMVs was studied on monolayers of Vero cells in six-well plates. Cells were infected with rMVs at an MOI of 0.1. At various time points post-infection, infected cells were scraped into 1 ml opti-MEM medium, lysed by freeze-thaw, clarified by centrifugation, and titered as described above.

MV Schwarz coded for the Schwarz measles vaccine strain and constituted the backbone of our MV vaccine platform. MV-SARS-CoV-2 candidate was produced before the study in our lab and expressed the stabilized pre-fusion form of Spike protein of SARS-CoV-2 virus.[48]

RT-PCR

To verify Pbfusion expression from the rMV construct, total RNA was extracted from infected Vero cells using the RNeasy Mini Kit (Qiagen). The cDNA synthesis and PCR steps were performed using the SuperScript IV One-Step RT-PCR System (Invitrogen) with primers targeting ATU3, according to the manufacturer's instructions. RT-PCR products were verified by Sanger sequencing (Eurofins Genomics). All primers used are described in Supplementary Table S2.

Mice experiments

Transgenic 129 sv mice expressing hCD46+ and IFNAR deficient were obtained from the Institut Pasteur animal facility. These mice have the same MHC haplotype than the classical C57BL/6 mice: MHC-I (H-2Kb/H-2 Db) and MHC-II (I-Ab) and they are susceptible to measles virus infection.

Adequate timing to isolate Trm cells is highly variable and depends on several factors as the model used, the studied microorganism or the vaccine platform used. We performed a kinetics experiment to determine an ideal timing to harvest the organs (7-14-21-days post immunization) after a single intraperitoneal immunization of 10^5 $TCID_{50}$ of MV Schwarz vaccine. Using a reduced number of animals (three per group), we determined that enough number of Trm cells were recovered twenty-one days after one single immunization and the percentage was not significantly different after two intraperitoneal immunizations (Supplementary table S3 and S4). The presented experiments were all made 21 days post immunization, except for the long-term experiment, which was conducted 90 days post-immunization.

To study liver and lung MV-specific resident memory CD8+ T cells, groups of 6 to 10-weeks old mice were immunized intraperitoneally with 10^5 $TCID_{50}$ of MV Schwarz or media vehicle (opti-MEM medium). Organs (liver, spleen, and lungs) were collected to assess the presence of tissue resident memory CD8+ T cells. To evaluate the influence of immunization routes, groups of 6 to 10-weeks old mice were immunized intraperitoneally, intramuscularly, intranasally or intravenously with 10^5 $TCID_{50}$ of MV and following organs collection, MV-specific tissue resident memory CD8+ T cells were studied in the liver, spleen, and lungs. To analyze SARS-CoV-2-specific responses, groups of 6 to 10-weeks old mice were immunized intranasally with 10^5 $TCID_{50}$ of MV-SARS-CoV-2 or with media vehicle (opti-MEM medium). Single cell suspensions were prepared from the lungs and the spleen and the tissue resident memory CD8+ T cells were assessed.

Organs collection and cells harvesting

Organs were harvested from mice at twenty-one days post-immunization and single cell suspension were prepared from liver, spleen, and lungs.

Spleens were collected and homogenized using a gentleMACS™ Dissociator (Miltenyi). Splenocytes were passed through a 70 µm mesh and red blood cells were lysed using the BD Pharm Lyse (BD Biosciences). After two washes with DPBS 1X (Gibco) 10% FBS (Corning), cells were resuspended in α-MEM media containing 10% FBS, 100 U/ml Penicillin-Streptomycin (Gibco), 10 mm HEPES (Gibco), 1 mm sodium pyruvate (Gibco), 2 mm L-Glutamine (Gibco), 50 µM β-mercaptoethanol (Sigma), and 0.1 mm non-essential amino acids (Gibco). Cells were maintained at 37°C in 5% CO_2 atmosphere until staining.

Livers were perfused via portal vein with 10 ml of saline sterile solution, then excised and maintained on ice in RPMI media (Gibco). The tissue was finely chopped and incubated for 30 minutes at 37°C with Collagenase IV (1 mg/ml, Gibco) and DNase I (10 U/ml, Roche) prepared in HBSS buffer with

Ca^{+2} and Mg^{+2}(Gibco). The liver tissue was homogenized using a gentleMACS™ Dissociator (Miltenyi). After enzymatic treatment, the cell suspension was filtered with a 100 µm mesh and red blood cells were lysed using the BD Pharm Lyse (BD Biosciences). The samples were centrifuged, and pellets were resuspended in 35% Percoll solution (Cytiva) in RPMI media (Gibco). After 30 minutes of centrifugation at 1360 g at room temperature with no brake, the pellet containing T cells was washed twice with RPMI 5% FBS and resuspended in α-MEM media (Gibco) containing 10% FBS, 100 U/ml Penicillin-Streptomycin (Gibco), 10 mm HEPES (Gibco), 1 mm sodium pyruvate (Gibco), 2 mm L-Glutamine (Gibco), 50 µM β-mercaptoethanol (Sigma), and 0.1 mm non-essential amino acids (Gibco). Cells were maintained at 37°C in 5% CO_2 atmosphere until staining.

Lungs were perfused with 20 ml of saline sterile solution with 10 U/ml of heparin (Sigma). The tissue was homogenized using a gentleMACS™ Dissociator (Miltenyi) and samples were filtered through a 70 µm mesh. Single cells suspensions were obtained using the Lung Dissociation Kit, mouse (Miltenyi) accordingly to manufacturer's instructions.

Flow cytometry analysis of mice samples

Two million cells from each organ per mouse were added per well of a V-bottom 96-well plates and stained as described below. Antibodies, supplier, clones, and dilutions employed are detailed in Supplementary Table S5.

To detect specific $CD8^+$ T cells we used the dextramer technology (Immudex). To identify specific-SARS-CoV-2 responses we used a previously described H2-D^b restricted epitope localized on the spike protein sequence: CVNFNFNGL ($S_{538-546}$). This immunodominant epitope captures approximatively 20% of the antigen-responding cells in an ELISPOT assay.[102] For MV specific responses, H2-D^b restricted epitope on Hemagglutinin protein was employed: RIVINREHL (H_{22-30}). This epitope captures around 2.5% of the total $CD8^+$ T cells in the spleen 10 days after immunization with wild-type measles virus.[103] We confirmed these results by an ELISPOT assay, where we identified about 2,000 IFN-γ-producing cells per 10^6 splenocytes after stimulation with H_{22-30} epitope 7 days after a single immunization with MV Schwarz. To recognize specific-Pbfusion responses we chose a H2-D^b restricted epitope (SCILNNMYF) contained in Pbfusion construct. We employed APC fluorochrome for MV dextramer and PE fluorochrome for Pbfusion and SARS-CoV-2 dextramers.

Liver-derived lymphocytes and splenocytes were incubated for 10 min with Mouse BD Fc Block (BD Biosciences) and then stained with MV and/or Pbfusion dextramer for 10 min according to manufacturer's instructions. Subsequently, cells were stained with CD3e FITC (BD Biosciences), CD8a (BD Biosciences), CD62L BV421 (BD Biosciences), CD69 PE-CF594 (BD Biosciences), CD11a PE-Cy7 (BD Biosciences), KLRG1 BV786 (BD Biosciences), CD183 BV605 (BioLegend), CD186 BV711 (Biolegend), and FVS 440 fixable viability stain (BD Biosciences) for 30 min at 4°C. After washing, cells were fixed with 2% formaldehyde (Sigma) in DPBS 1X for 15 minutes at 4°C.

Lung-derived lymphocytes and splenocytes were incubated for 10 min with Mouse BD Fc Block (BD Biosciences) and then stained with MV and/or SARS-CoV-2 dextramer for 10 min according to manufacturer's instructions. Subsequently, cells were stained with CD3e FITC (BD Biosciences), CD8a (BD Biosciences), CD62L BV421 (BD Biosciences), CD69 PE-CF594 (BD Biosciences), CD4 BV786 (BD Biosciences), CD183 BV605 (BioLegend), CD49a BV711 (BD Biosciences), CD103 PE (BD Biosciences), CD44 APC-R700 (BD Biosciences), and FVS 440 fixable viability stain (BD Biosciences) for 30 min at 4°C. After washing, cells were fixed with 2% formaldehyde (Sigma) in DPBS 1X for 15 minutes at 4°C.

Mouse data were acquired on a FACSymphony (Becton Dickinson). Data were analyzed using FlowJo software (Becton, Dickinson and Company, version 10.8.1). The gating strategy and the controls (FMO and isotypes) are shown in Supplementary Fig. S2A (liver panel) and S2B (lung panel).

Intracellular cytokine staining

Freshly extracted lung-derived lymphocytes from immunized mice were analyzed by flow cytometry for their capacity to secrete IFN-γ, Granzyme B and TNF-α upon specific stimulation. Cells were cultured in U-bottom 96-well plates (2.0×10^6 cells/well) in a volume of 0.2 ml complete medium (MEM— 10% FCS supplemented with non-essential amino-acids 1%, sodium pyruvate 1%, and β-mercapto-ethanol). Cells were stimulated for 16 h at 37°C with PMA/ionomycin (#00–4970, ebioscience) as positive control, complete MEM as negative control, and live attenuated MV-Schwarz virus at an MOI of 1. Brefeldin A (#B6542, Sigma) at 10 µg/ml was added to the culture medium 4 h after the beginning of the stimulation. Stimulated cells were incubated for 10 min with Mouse BD Fc Block (BD Biosciences) and then stained with MV dextramer for 10 min according to manufacturer's instructions. Subsequently, cells were stained with CD3e FITC (BD Biosciences), CD8a (BD Biosciences), CD62L BV421 (BD Biosciences), CD69 PE-CF594 (BD Biosciences), CD4 BV786 (BD Biosciences), CD183 BV605 (BioLegend), CD49a BV711 (BD Biosciences), CD103 PE-Cy7 (BD Biosciences), CD44 APC-R700 (BD Biosciences), and FVS 440 fixable viability stain (BD Biosciences) for 30 min at 4°C. After washing, cells were fixed and permeabilized with BD Fixation/Permeabilization kit (BD Biosciences) and stained with TNF-α BB700 (BD Biosciences) Granzyme B PE (BioLegend) and IFN-γ BUV737 (BD Biosciences) for 30 min in the dark. Mouse data were acquired on a FACSymphony (Becton Dickinson). Data were analyzed using FlowJo software (Becton, Dickinson and Company, version 10.8.1). The gating strategy and the controls (FMO and unstimulated cells) are shown in Supplementary Fig. S3. As the studied population was very low (0.1–0.2%), bright fluorophores were used to detect MV-specificity and the intracellular cytokines. The gating was first done using FMO then adjusted using positive controls (PMA/ionomycin stimulated cells) and negative controls (unstimulated samples) from the control group to define a reasonable β. Finally, the unvaccinated control group defined the background noise for statistical analysis.

Isolation of human PBMCs and flow cytometry analysis

Human peripheral blood mononuclear cells were obtained from whole blood using LymphoPrep Tube (Progen) and were immediately cryopreserved. After thawing, the cell viability (Trypan Blue) was >2%. Cells were resuspended in RPMI 1640 supplemented with 10% FBS (Corning), 100 U/ml Penicillin-Streptomycin (Gibco), 1 mm sodium pyruvate (Gibco), 2 mm L-Glutamine (Gibco), 50 μM β-mercaptoethanol (Sigma), and 0.1 mm non-essential amino acids (Gibco).

One million cells per individual were added per well in a U-bottom 96-well plates. Human PBMCs were stimulated for 20 hours with MV Schwarz UV-inactivated vaccine strain (MOI of 1), Wuhan SARS-CoV-2 UV-inactivated virus (MOI of 1) or unstimulated (media culture alone). Plates were incubated on ice for 15 min to stop the stimulation and subsequently transferred to a V-bottom 96-well plates. Stimulated cells were incubated separately with two different antibody mix combinations. One plate was incubated with FcR Blocking Reagent for 10 min and stained with CD3 VioGreen (Miltenyi), CD4 PerCP (Miltenyi), CD8 APC-Cy7 (Miltenyi), CD45RO BV605 (BD Biosciences), CD69 VioBright B515 (Miltenyi), CD62L VioBright R720 (Miltenyi), CD197 VioBlue (Miltenyi), CCR10 PE (Miltenyi), CXCR5 PE Vio615 (Miltenyi), CCR9 PE-Cy7 (Miltenyi), CCR4 APC (Miltenyi), Live/Dead fixable blue (UV 450) (Thermofisher) for 10 min at 4°C. After washing, cells were fixed with 4% paraformaldehyde in DPBS 1X for 15 minutes at 4°C.

The second plate was incubated with FcR Blocking Reagent for 10 min and stained with CD3 VioGreen (Miltenyi), CD4 PerCP (Miltenyi), CD8 APC-Cy7 (Miltenyi), CD45RO BV605 (BD Biosciences), CD69 VioBright B515 (Miltenyi), CD62L VioBright R720 (Miltenyi), CD196 VioBlue (Miltenyi), CD186 PE (Miltenyi), CXCR3 PE Vio615 (Miltenyi), CD103 PE-Cy7 (Miltenyi), CD161 APC (Miltenyi), Live/Dead fixable blue (UV 450) (Thermofisher) for 10 min at 4°C. After washing, cells were fixed with 4% paraformaldehyde in DPBS 1X for 15 minutes at 4°C.

Human PBMCs data were acquired on a Cytoflex Lx (Beckman Coulter). Data were analyzed using FlowJo software (Becton, Dickinson and Company, version 10.8.1). The gating strategy and the controls (FMO) are shown in Supplementary Fig. S4A (human PBMCs mix 1) and S4B (human PBMCs mix 2).

Statistical analysis

Statistical analyses were performed using R (version 4.2.1) and R Studio (version 2022.07.1 + 554) softwares. The statistical tests used are indicated in each figure legend.

For mice experiment: when comparing two independent conditions, the Mann-Whitney-Wilcoxon test was used. For multiple comparisons, the non-parametric Kruskal – Wallis test was employed. Then, pairwise comparisons between groups were calculated using Dunn test and p-values were adjusted applying the Benjamini-Hochberg correction. Results were considered significant if adjusted $p < 0.05$.

For human experiment: to determine MV-stimulated-induced changes in the expression of homing receptors, we carried out a univariate analysis for each marker, comparing both stimulations with the Wilcoxon-Mann-Whitney test. After calculating p-values for immune parameters in the datasets, a correction for multiple comparisons was made using the Benjamini – Hochberg correction. Immune measures in which comparison data showed a significant difference at $p < 0.05$ and a false discovery rate fdr < 0.20 were selected.

Disclosure statement

No potential conflict of interest was reported by the author(s).

Notes on contributor

Marie Mura is a military MD, PhD, and specialist in vaccinology. Her scientific background includes preclinical development of a malaria vaccine on a murine model using a measles viral vector at the Pasteur Institute, as well as immunoprofiling human vaccine responses in a phase I clinical trial with an infectious challenge at the Walter Reed Army Institute of Research. Since 2021, she has been leading the Host-Pathogen Interactions Unit in the Microbiology and Infectious Diseases Department at the Institut de Recherche Biomédicale des Armées. Her research focuses on integrated immune memories and tropism of vaccine responses to enhance the development of new vaccines.

ORCID

Marie Mura http://orcid.org/0000-0003-0051-3773

Author contributions

All authors attest they meet the ICMJE criteria for authorship. Conceptualization, HVP, FT, JNT, MM; methodology, HVP, MM, CR, MB, CC, PF, VN; software, HVP; formal analysis, HVP, MM; investigation, HVP, MM; writing-original draft preparation, HVP; writing – review and editing, FT, JNT, MM; All authors have read and agreed to the published version of the manuscript.

References

1. Benn CS, Aaby P. Measles vaccination and reduced child mortality: prevention of immune amnesia or beneficial non-specific

effects of measles vaccine? J Infect. 2023;87(4):295–304. doi:10.1016/j.jinf.2023.07.010.

2. Goodson JL, Seward JF. Measles 50 years after use of measles vaccine. Infect Dis Clin N Am. 2015;29(4):725–743. doi:10.1016/j.idc.2015.08.001.

3. Griffin DE. Measles vaccine. Viral Immunol. 2018;31(2):86–95. doi:10.1089/vim.2017.0143.

4. Lin WH, Griffin DE, Rota PA, Papania M, Cape SP, Bennett D, Quinn B, Sievers RE, Shermer C, Powell K, et al. Successful respiratory immunization with dry powder live-attenuated measles virus vaccine in rhesus macaques. Proc Natl Acad Sci USA. 2011;108(7):2987–2992. doi:10.1073/pnas.1017334108.

5. Bolotin S, Hughes SL, Gul N, Khan S, Rota PA, Severini A, Hahné S, Tricco A, Moss WJ, Orenstein W, et al. What is the evidence to support a correlate of protection for measles? A systematic review. J Infect Dis. 2020;221(10):1576–1583. doi:10.1093/infdis/jiz380.

6. Griffin DE. The immune response in measles: virus control, clearance and protective immunity. Viruses. 2016;8(10):282. doi:10.3390/v8100282.

7. Chen RT, Markowitz LE, Albrecht P, Stewart JA, Mofenson LM, Preblud SR, Orenstein WA. Measles antibody: reevaluation of protective titers. J Infect Dis. 1990;162(5):1036–1042. doi:10.1093/infdis/162.5.1036.

8. Good RA, Zak SJ. Disturbances in gamma globulin synthesis as experiments of nature. Pediatrics. 1956;18(1):109–149. doi:10.1542/peds.18.1.109.

9. Burnet FM. Measles as an index of immunological function. Lancet. 1968;2(7568):610–613. doi:10.1016/s0140-6736(68)90701-0.

10. Markowitz LE, Chandler FW, Roldan EO, Saldana MJ, Roach KC, Hutchins SS, Preblud SR, Mitchell CD, Scott GB. Fatal measles pneumonia without rash in a child with AIDS. J Infect Dis. 1988;158(2):480–483. doi:10.1093/infdis/158.2.480.

11. Mitus A, Holloway A, Evans AE, Enders JF. Attenuated measles vaccine in children with acute leukemia. Am J Dis Child. 1962;103(3):413–418. doi:10.1001/archpedi.1962.02080020425051.

12. Lin WH, Pan CH, Adams RJ, Laube BL, Griffin DE. Vaccine-induced measles virus-specific T cells do not prevent infection or disease but facilitate subsequent clearance of viral RNA. mBio. 2014;5(2):e01047. doi:10.1128/mBio.01047-14.

13. Ovsyannikova IG, Dhiman N, Jacobson RM, Vierkant RA, Poland GA. Frequency of measles virus-specific CD4+ and CD8+ T cells in subjects seronegative or highly seropositive for measles vaccine. Clin Diagn Lab Immunol. 2003;10(3):411–416. doi:10.1128/cdli.10.3.411-416.2003.

14. Naniche D, Garenne M, Rae C, Manchester M, Buchta R, Brodine SK, Oldstone M. Decrease in measles virus–specific CD4 T cell memory in vaccinated subjects. J Infect Dis. 2004;190(8):1387–1395. doi:10.1086/424571.

15. Schenkel JM, Masopust D. Tissue-resident memory T cells. Immunity. 2014;41(6):886–897. doi:10.1016/j.immuni.2014.12.007.

16. Crowl JT, Heeg M, Ferry A, Milner JJ, Omilusik KD, Toma C, He Z, Chang JT, Goldrath AW. Tissue-resident memory CD8(+) T cells possess unique transcriptional, epigenetic and functional adaptations to different tissue environments. Nat Immunol. 2022;23(7):1121–1131. doi:10.1038/s41590-022-01229-8.

17. Simms PE, Ellis TM. Utility of flow cytometric detection of CD69 expression as a rapid method for determining poly- and oligoclonal lymphocyte activation. Clin Diagn Lab Immunol. 1996;3(3):301–304. doi:10.1128/cdli.3.3.301-304.1996.

18. Sathaliyawala T, Kubota M, Yudanin N, Turner D, Camp P, Thome JJ, Bickham K, Lerner H, Goldstein M, Sykes M, et al. Distribution and compartmentalization of human circulating and tissue-resident memory T cell subsets. Immunity. 2013;38(1):187–197. doi:10.1016/j.immuni.2012.09.020.

19. Mackay LK, Rahimpour A, Ma JZ, Collins N, Stock AT, Hafon ML, Vega-Ramos J, Lauzurica P, Mueller SN, Stefanovic T, et al. The developmental pathway for CD103(+)CD8+ tissue-resident memory T cells of skin. Nat Immunol. 2013;14(12):1294–1301. doi:10.1038/ni.2744.

20. Bromley SK, Akbaba H, Mani V, Mora-Buch R, Chasse AY, Sama A, Luster AD. CD49a regulates cutaneous resident memory CD8+ T cell persistence and response. Cell Rep. 2020;32(9):108085. doi:10.1016/j.celrep.2020.108085.

21. McNamara HA, Cai Y, Wagle MV, Sontani Y, Roots CM, Miosge LA, O'Connor JH, Sutton HJ, Ganusov VV, Heath WR, et al. Up-regulation of LFA-1 allows liver-resident memory T cells to patrol and remain in the hepatic sinusoids. Sci Immunol. 2017;2(9):2. doi:10.1126/sciimmunol.aaj1996.

22. Yang K, Kallies A. Tissue-specific differentiation of CD8(+) resident memory T cells. Trends Immunol. 2021;42(10):876–890. doi:10.1016/j.it.2021.08.002.

23. Paik DH, Farber DL. Anti-viral protective capacity of tissue resident memory T cells. Curr Opin Virol. 2021;46:20–26. doi:10.1016/j.coviro.2020.09.006.

24. Dijkgraaf FE, Kok L, Schumacher TNM. Formation of tissue-resident CD8 + T-Cell memory. Cold Spring Harb Perspect Biol. 2021;13(8):13. doi:10.1101/cshperspect.a038117.

25. Hirahara K, Kokubo K, Aoki A, Kiuchi M, Nakayama T. The role of CD4(+) resident memory T cells in local immunity in the mucosal tissue - protection versus pathology. Front Immunol. 2021;12:616309. doi:10.3389/fimmu.2021.616309.

26. Turner DL, Farber DL. Mucosal resident memory CD4 T cells in protection and immunopathology. Front Immunol. 2014;5:331. doi:10.3389/fimmu.2014.00331.

27. Campbell DJ, Butcher EC. Rapid acquisition of tissue-specific homing phenotypes by CD4 + T cells activated in cutaneous or mucosal lymphoid tissues. J Exp Med. 2002;195(1):135–141. doi:10.1084/jem.20011502.

28. Dudda JC, Simon JC, Martin S. Dendritic cell immunization route determines CD8+ T cell trafficking to inflamed skin: role for tissue microenvironment and dendritic cells in establishment of T cell-homing subsets. J Immunol. 2004;172(2):857–863. doi:10.4049/jimmunol.172.2.857.

29. Teijaro JR, Turner D, Pham Q, Wherry EJ, Lefrançois L, Farber DL. Cutting edge: tissue-retentive lung memory CD4 T cells mediate optimal protection to respiratory virus infection. J Immunol. 2011;187(11):5510–5514. doi:10.4049/jimmunol.1102243.

30. Mura M, Atre T, Savransky T, Bergmann-Leitner ES. Differential homing receptor profiles of lymphocytes induced by attenuated versus live Plasmodium falciparum sporozoites. Vaccines (Basel). 2022;10(10):1768. doi:10.3390/vaccines10101768.

31. Zens KD, Chen JK, Farber DL. Vaccine-generated lung tissue–resident memory T cells provide heterosubtypic protection to influenza infection. JCI Insight. 2016;1(10):1. doi:10.1172/jci.insight.85832.

32. McMaster SR, Wilson JJ, Wang H, Kohlmeier JE. Airway-resident memory CD8 T cells provide antigen-specific protection against respiratory virus challenge through rapid IFN-γ production. J Immunol. 2015;195(1):203–209. doi:10.4049/jimmunol.1402975.

33. Seder RA, Darrah PA, Roederer M. T-cell quality in memory and protection: implications for vaccine design. Nat Rev Immunol. 2008;8(4):247–258. doi:10.1038/nri2274.

34. Koutsakos M, Illing PT, Nguyen THO, Mifsud NA, Crawford JC, Rizzetto S, Eltahla AA, Clemens EB, Sant S, Chua BY, et al. Human CD8(+) T cell cross-reactivity across influenza A, B and C viruses. Nat Immunol. 2019;20(5):613–625. doi:10.1038/s41590-019-0320-6.

35. Jozwik A, Habibi MS, Paras A, Zhu J, Guvenel A, Dhariwal J, Almond M, Wong EHC, Sykes A, Maybeno M, et al. Rsv-specific airway resident memory CD8+ T cells and differential disease severity after experimental human infection. Nat Commun. 2015;6(1):10224. doi:10.1038/ncomms10224.

36. Retamal-Diaz A, Covian C, Pacheco GA, Castiglione-Matamala AT, Bueno SM, Gonzalez PA, Kalergis AM. Contribution of resident memory CD8(+) T cells to protective immunity against respiratory syncytial virus and their impact on vaccine design. Pathogens. 2019;8(3):147. doi:10.3390/pathogens8030147.

37. Uddbäck I, Michalets SE, Saha A, Mattingly C, Kost KN, Williams ME, Lawrence LA, Hicks SL, Lowen AC, Ahmed H,

et al. Prevention of respiratory virus transmission by resident memory CD8(+) T cells. Nature. 2024;626(7998):392–400. doi:10.1038/s41586-023-06937-1.

38. Fernandez-Ruiz D, de Menezes MN, Holz LE, Ghilas S, Heath WR, Beattie L. Harnessing liver-resident memory T cells for protection against malaria. Expert Rev Vaccines. 2021;20(2):127–141. doi:10.1080/14760584.2021.1881485.

39. Cheng Y, Gunasegaran B, Singh HD, Dutertre CA, Loh CY, Lim JQ, Crawford JC, Lee HK, Zhang X, Lee B, et al. Non-terminally exhausted tumor-resident memory hbv-specific T cell responses correlate with relapse-free survival in hepatocellular carcinoma. Immunity. 2021;54(8):1825–1840.e7. doi:10.1016/j.immuni.2021.06.013.

40. Shoukry NH, Grakoui A, Houghton M, Chien DY, Ghrayeb J, Reimann KA, Walker CM. Memory CD8+ T cells are required for protection from persistent hepatitis C virus infection. J Exp Med. 2003;197(12):1645–1655. doi:10.1084/jem.20030239.

41. Combredet C, Labrousse V, Mollet L, Lorin C, Delebecque F, Hurtrel B, McClure H, Feinberg MB, Brahic M, Tangy F, et al. A molecularly cloned Schwarz strain of measles virus vaccine induces strong immune responses in macaques and transgenic mice. J Virol. 2003;77(21):11546–11554. doi:10.1128/jvi.77.21.11546-11554.2003.

42. Ramsauer K, Schwameis M, Firbas C, Mullner M, Putnak RJ, Thomas SJ, Desprès P, Tauber E, Jilma B, Tangy F, et al. Immunogenicity, safety, and tolerability of a recombinant measles-virus-based chikungunya vaccine: a randomised, double-blind, placebo-controlled, active-comparator, first-in-man trial. Lancet Infect Dis. 2015;15(5):519–527. doi:10.1016/S1473-3099(15)70043-5.

43. Reisinger EC, Tschismarov R, Beubler E, Wiedermann U, Firbas C, Loebermann M, Pfeiffer A, Muellner M, Tauber E, Ramsauer K, et al. Immunogenicity, safety, and tolerability of the measles-vectored chikungunya virus vaccine MV-CHIK: a double-blind, randomised, placebo-controlled and active-controlled phase 2 trial. Lancet. 2019;392(10165):2718–2727. doi:10.1016/S0140-6736(18)32488-7.

44. Guerbois M, Moris A, Combredet C, Najburg V, Ruffie C, Février M, Cayet N, Brandler S, Brandler O, Tangy F. Live attenuated measles vaccine expressing HIV-1 Gag virus like particles covered with gp160ΔV1V2 is strongly immunogenic. Virology. 2009 May 25;388(1):191–203. doi:10.1016/j.virol.2009.02.047.

45. Frantz PN, Teeravechyan S, Tangy F. Measles-derived vaccines to prevent emerging viral diseases. Microbes Infect. 2018;20(9–10):493–500. doi:10.1016/j.micinf.2018.01.005.

46. Mateo M, Reynard S, Journeaux A, Germain C, Hortion J, Carnec X, Picard C, Baillet N, Borges-Cardoso V, Merabet O, et al. A single-shot Lassa vaccine induces long-term immunity and protects cynomolgus monkeys against heterologous strains. Sci Transl Med. 2021;13(597):13. doi:10.1126/scitranslmed.abf6348.

47. Mura M, Ruffie C, Combredet C, Aliprandini E, Formaglio P, Chitnis CE, Amino R, Tangy F. Recombinant measles vaccine expressing malaria antigens induces long-term memory and protection in mice. NPJ Vaccines. 2019;4(1):12. doi:10.1038/s41541-019-0106-8.

48. Frantz PN, Barinov A, Ruffie C, Combredet C, Najburg V, de Melo GD, Larrous F, Kergoat L, Teeravechyan S, Jongkaewwattana A, et al. A live measles-vectored COVID-19 vaccine induces strong immunity and protection from SARS-CoV-2 challenge in mice and hamsters. Nat Commun. 2021;12(1):6277. doi:10.1038/s41467-021-26506-2.

49. Amino R, Charneau P, Blanc C, Lagal V. Malaria pre-erythrocytic antigens as a fusion polypeptide and their use in the elicitation of a protective immune response in a host. 2019; WO2019224606A1.

50. Brinkman CC, Peske JD, Engelhard VH. Peripheral tissue homing receptor control of naive, effector, and memory CD8 T cell localization in lymphoid and non-lymphoid tissues. Front Immunol. 2013;4:241. doi:10.3389/fimmu.2013.00241.

51. Tubo NJ, McLachlan JB, Campbell JJ. Chemokine receptor requirements for epidermal T-cell trafficking. Am J Pathol. 2011;178(6):2496–2503. doi:10.1016/j.ajpath.2011.02.031.

52. Sigmundsdottir H, Pan J, Debes GF, Alt C, Habtezion A, Soler D, Butcher EC. DCs metabolize sunlight-induced vitamin D3 to 'program' T cell attraction to the epidermal chemokine CCL27. Nat Immunol. 2007;8:285–293. doi:10.1038/ni1433.

53. Chu F, Li HS, Liu X, Cao J, Ma W, Ma Y, Weng J, Zhu Z, Cheng X, Wang Z, et al. CXCR5(+)CD8(+) T cells are a distinct functional subset with an antitumor activity. Leukemia. 2019;33(11):2640–2653. doi:10.1038/s41375-019-0464-2.

54. Mora JR, Bono MR, Manjunath N, Weninger W, Cavanagh LL, Rosemblatt M, Von Andrian UH. Selective imprinting of gut-homing T cells by Peyer's patch dendritic cells. Nature. 2003;424(6944):88–93. doi:10.1038/nature01726.

55. Papadakis KA, Landers C, Prehn J, Kouroumalis EA, Moreno ST, Gutierrez-Ramos JC, Hodge MR, Targan SR. CC chemokine receptor 9 expression defines a subset of peripheral blood lymphocytes with mucosal T cell phenotype and Th1 or T-regulatory 1 cytokine profile. J Immunol. 2003;171(1):159–165. doi:10.4049/jimmunol.171.1.159.

56. Campbell JJ, O'Connell DJ, Wurbel MA. Cutting edge: chemokine receptor CCR4 is necessary for antigen-driven cutaneous accumulation of CD4 T cells under physiological conditions. J Immunol. 2007;178(6):3358–3362. doi:10.4049/jimmunol.178.6.3358.

57. Ito T, Carson W, Cavassani KA, Connett JM, Kunkel SL. CCR6 as a mediator of immunity in the lung and gut. Exp Cell Res. 2011;317(5):613–619. doi:10.1016/j.yexcr.2010.12.018.

58. Tse SW, Radtke AJ, Espinosa DA, Cockburn IA, Zavala F. The chemokine receptor CXCR6 is required for the maintenance of liver memory CD8(+) T cells specific for infectious pathogens. J Infect Dis. 2014;210(9):1508–1516. doi:10.1093/infdis/jiu281.

59. Wein AN, McMaster SR, Takamura S, Dunbar PR, Cartwright EK, Hayward SL, McManus DT, Shimaoka T, Ueha S, Tsukui T, et al. CXCR6 regulates localization of tissue-resident memory CD8 T cells to the airways. J Exp Med. 2019;216(12):2748–2762. doi:10.1084/jem.20181308.

60. Groom JR. Regulators of T-cell fate: integration of cell migration, differentiation and function. Immunol Rev. 2019;289(1):101–114. doi:10.1111/imr.12742.

61. Topham DJ, Reilly EC. Tissue-resident memory CD8(+) T cells: from phenotype to function. Front Immunol. 2018;9:515. doi:10.3389/fimmu.2018.00515.

62. Konduri V, Oyewole-Said D, Vazquez-Perez J, Weldon SA, Halpert MM, Levitt JM, Decker WK. CD8(+)CD161(+) T-Cells: cytotoxic memory cells with high therapeutic potential. Front Immunol. 2020;11:613204. doi:10.3389/fimmu.2020.613204.

63. Siracusa F, Durek P, McGrath MA, Sercan-Alp Ö, Rao A, Du W, Cendón C, Chang H-D, Heinz GA, Mashreghi M-F, et al. CD69+ memory T lymphocytes of the bone marrow and spleen express the signature transcripts of tissue-resident memory T lymphocytes. Eur J Immunol. 2019;49(6):966–968. doi:10.1002/eji.201847982.

64. Hassert M, Harty JT. Tissue resident memory T cells- a new benchmark for the induction of vaccine-induced mucosal immunity. Front Immunol. 2022;13:13. doi:10.3389/fimmu.2022.1039194.

65. Varese A, Nakawesi J, Farias A, Kirsebom FCM, Paulsen M, Nuriev R, Johansson C. Type I interferons and MAVS signaling are necessary for tissue resident memory CD8+ T cell responses to RSV infection. PLOS Pathog. 2022;18(2):e1010272. doi:10.1371/journal.ppat.1010272.

66. Mura M, Ruffie C, Billon-Denis E, Combredet C, Tournier JN, Tangy F. hCD46 receptor is not required for measles vaccine Schwarz strain replication in vivo: type-I IFN is the species barrier in mice. Virology. 2018;524:151–159. doi:10.1016/j.virol.2018.08.014.

67. Oja AE, Piet B, Helbig C, Stark R, van der Zwan D, Blaauwgeers H, Remmerswaal EBM, Amsen D, Jonkers RE, Moerland PD, et al. Trigger-happy resident memory CD4(+) T cells inhabit the human lungs. Mucosal Immunol. 2018;11(3):654–667. doi:10.1038/mi.2017.94.

68. Zhang Y, Chamblee M, Xu J, Qu P, Shamseldin MM, Yoo SJ, Misny J, Thongpan I, Kc M, Hall JM, et al. Three SARS-CoV-2 spike protein variants delivered intranasally by measles and mumps vaccines are broadly protective. Nat Commun. 2024;15 (1):5589. doi:10.1038/s41467-024-49443-2.

69. Rosato PC, Beura LK, Masopust D. Tissue resident memory T cells and viral immunity. Curr Opin Virol. 2017;22:44–50. doi:10.1016/ j.coviro.2016.11.011.

70. Rotrosen E, Kupper TS. Assessing the generation of tissue resident memory T cells by vaccines. Nat Rev Immunol. 2023;23 (10):655–665. doi:10.1038/s41577-023-00853-1.

71. Baeza Garcia A, Siu E, Sun T, Exler V, Brito L, Hekele A, Otten G, Augustijn K, Janse CJ, Ulmer JB, et al. Neutralization of the plasmodium-encoded MIF ortholog confers protective immunity against malaria infection. Nat Commun. 2018;9(1):2714. doi:10. 1038/s41467-018-05041-7.

72. Welten SPM, Oderbolz J, Yilmaz V, Bidgood SR, Gould V, Mercer J, Spörri R, Oxenius A. Influenza- and mcmv-induced memory CD8 T cells control respiratory vaccinia virus infection despite residence in distinct anatomical niches. Mucosal Immunol. 2021;14(3):728–742. doi:10.1038/s41385-020-00373-4.

73. Shahnaij M, Iyori M, Mizukami H, Kajino M, Yamagoshi I, Syafira I, Yusuf Y, Fujiwara K, Yamamoto DS, Kato H, et al. Liver-directed AAV8 booster vaccine expressing Plasmodium falciparum antigen following adenovirus vaccine priming elicits sterile protection in a murine model. Front Immunol. 2021;12:612910. doi:10.3389/fimmu.2021.612910.

74. Takamura S. Niches for the long-term maintenance of tissue-resident memory T cells. Front Immunol. 2018;9:1214. doi:10.3389/fimmu.2018.01214.

75. Takamura S, Yagi H, Hakata Y, Motozono C, McMaster SR, Masumoto T, Fujisawa M, Chikaishi T, Komeda J, Itoh J, et al. Specific niches for lung-resident memory CD8+ T cells at the site of tissue regeneration enable CD69-independent maintenance. J Exp Med. 2016;213(13):3057–3073. doi:10.1084/jem.20160938.

76. Wu T, Hu Y, Lee YT, Bouchard KR, Benechet A, Khanna K, Cauley LS. Lung-resident memory CD8 T cells (TRM) are indispensable for optimal cross-protection against pulmonary virus infection. J Leukoc Biol. 2014;95(2):215–224. doi:10.1189/jlb. 0313180.

77. Luangrath MA, Schmidt ME, Hartwig SM, Varga SM. Tissue-resident memory T cells in the lungs protect against acute respiratory syncytial virus infection. Immunohorizons. 2021;5(2):59–69. doi:10.4049/immunohorizons.2000067.

78. Uddback I, Cartwright EK, Scholler AS, Wein AN, Hayward SL, Lobby J, Takamura S, Thomsen AR, Kohlmeier JE, Christensen JP, et al. Long-term maintenance of lung resident memory T cells is mediated by persistent antigen. Mucosal Immunol. 2021;14 (1):92–99. doi:10.1038/s41385-020-0309-3.

79. Myers RM, Greiner SM, Harvey ME, Griesmann G, Kuffel MJ, Buhrow SA, Reid JM, Federspiel M, Ames MM, Dingli D, et al. Preclinical pharmacology and toxicology of intravenous MV-NIS, an oncolytic measles virus administered with or without cyclophosphamide. Clin Pharmacol Ther. 2007;82(6):700–710. doi:10.1038/sj.clpt.6100409.

80. Reilly EC, Sportiello M, Emo KL, Amitrano AM, Jha R, Kumar ABR, Laniewski NG, Yang H, Kim M, Topham DJ, et al. CD49a identifies polyfunctional memory CD8 T cell subsets that persist in the lungs after influenza infection. Front Immunol. 2021;12:728669. doi:10.3389/fimmu.2021.728669.

81. Lobby JL, Uddback I, Scharer CD, Mi T, Boss JM, Thomsen AR, Christensen JP, Kohlmeier JE. Persistent antigen harbored by alveolar macrophages enhances the maintenance of lung-resident memory CD8(+) T cells. J Immunol. 2022;209(9):1778–1787. doi:10.4049/jimmunol.2200082.

82. Borges da Silva H, Wang H, Qian LJ, Hogquist KA, Jameson SC. ARTC2.2/P2RX7 signaling during cell isolation distorts function

and quantification of tissue-resident CD8(+) T cell and invariant NKT subsets. J Immunol. 2019;202(7):2153–2163. doi:10.4049/jim munol.1801613.

83. Epstein JE, Tewari K, Lyke KE, Sim BK, Billingsley PF, Laurens MB, Gunasekera A, Chakravarty S, James ER, Sedegah M, et al. Live attenuated malaria vaccine designed to protect through hepatic CD8 + T cell immunity. Science. 2011;334(6055):475–480. doi:10.1126/science.1211548.

84. Weiss WR, Jiang CG, Gruner AC. Protective CD8+ T lymphocytes in primates immunized with malaria sporozoites. PLOS ONE. 2012;7(2):e31247. doi:10.1371/journal.pone.0031247.

85. Ishizuka AS, Lyke KE, DeZure A, Berry AA, Richie TL, Mendoza FH, Enama ME, Gordon IJ, Chang L-J, Sarwar UN, et al. Protection against malaria at 1 year and immune correlates following PfSPZ vaccination. Nat Med. 2016;22(6):614–623. doi:10.1038/nm.4110.

86. Fernandez-Ruiz D, Ng WY, Holz LE, Ma JZ, Zaid A, Wong YC, Lau L, Mollard V, Cozijnsen A, Collins N, et al. Liver-resident memory CD8(+) T cells form a front-line defense against malaria liver-stage infection. Immunity. 2016;45(4):889–902. doi:10.1016/ j.immuni.2016.08.011.

87. Zheng X, Oduro JD, Boehme JD, Borkner L, Ebensen T, Heise U, Gereke M, Pils MC, Krmpotic A, Guzmán CA, et al. Mucosal CD8 + T cell responses induced by an MCMV based vaccine vector confer protection against influenza challenge. PLOS Pathog. 2019;15(9):e1008036. doi:10.1371/journal.ppat.1008036.

88. Ku MW, Bourgine M, Authie P, Lopez J, Nemirov K, Moncoq F, Noirat A, Vesin B, Nevo F, Blanc C, et al. Intranasal vaccination with a lentiviral vector protects against SARS-CoV-2 in preclinical animal models. Cell Host Microbe. 2021;29(2):236–249.e6. doi:10. 1016/j.chom.2020.12.010.

89. Bosnjak B, Odak I, Barros-Martins J, Sandrock I, Hammerschmidt SI, Permanyer M, Patzer GE, Georgiev H, Gutierrez Jauregui R, Tscherne A, et al. Intranasal delivery of MVA vector vaccine induces effective pulmonary immunity against SARS-CoV-2 in rodents. Front Immunol. 2021;12:772240. doi:10.3389/fimmu.2021.772240.

90. Morabito KM, Ruckwardt TJ, Bar-Haim E, Nair D, Moin SM, Redwood AJ, Price DA, Graham BS. Memory inflation drives tissue-resident memory CD8(+) T cell maintenance in the lung after intranasal vaccination with murine cytomegalovirus. Front Immunol. 2018;9:1861. doi:10.3389/fimmu.2018.01861.

91. de Swart RL, de Vries RD, Rennick LJ, van Amerongen G, McQuaid S, Verburgh RJ, Yüksel S, de Jong A, Lemon K, Nguyen DT, et al. Needle-free delivery of measles virus vaccine to the lower respiratory tract of non-human primates elicits optimal immunity and protection. NPJ Vaccines. 2017;2(1):22. doi:10. 1038/s41541-017-0022-8.

92. Jeyanathan M, Fritz DK, Afkhami S, Aguirre E, Howie KJ, Zganiacz A, Dvorkin-Gheva A, Thompson MR, Silver RF, Cusack RP, et al. Aerosol delivery, but not intramuscular injection, of adenovirus-vectored tuberculosis vaccine induces respiratory-mucosal immunity in humans. JCI Insight. 2022;7 (3):7. doi:10.1172/jci.insight.155655.

93. Szabo PA, Dogra P, Gray JI, Wells SB, Connors TJ, Weisberg SP, Krupska I, Matsumoto R, Poon MML, Idzikowski E, et al. Longitudinal profiling of respiratory and systemic immune responses reveals myeloid cell-driven lung inflammation in severe COVID-19. Immunity. 2021;54(4):797–814.e6. doi:10.1016/j. immuni.2021.03.005.

94. Pallett LJ, Burton AR, Amin OE, Rodriguez-Tajes S, Patel AA, Zakeri N, Jeffery-Smith A, Swadling L, Schmidt NM, Baiges A, et al. Longevity and replenishment of human liver-resident memory T cells and mononuclear phagocytes. J Exp Med. 2020;217 (9):217. doi:10.1084/jem.20200050.

95. Pallett LJ, Davies J, Colbeck EJ, Robertson F, Hansi N, Easom NJW, Burton AR, Stegmann KA, Schurich A, Swadling L,

et al. IL-2(high) tissue-resident T cells in the human liver: sentinels for hepatotropic infection. J Exp Med. 2017;214(6):1567–1580. doi:10.1084/jem.20162115.

96. Okhrimenko A, Grün JR, Westendorf K, Fang Z, Reinke S, von Roth P, Wassilew G, Kühl AA, Kudernatsch R, Demski S, et al. Human memory T cells from the bone marrow are resting and maintain long-lasting systemic memory. Proc Natl Acad Sci USA. 2014;111(25):9229–9234. doi:10.1073/pnas.1318731111.

97. Mabrouk N, Tran T, Sam I, Pourmir I, Gruel N, Granier C, Pineau J, Gey A, Kobold S, Fabre E, et al. CXCR6 expressing T cells: functions and role in the control of tumors. Front Immunol. 2022;13:1022136. doi:10.3389/fimmu.2022.1022136.

98. Sato T, Thorlacius H, Johnston B, Staton TL, Xiang W, Littman DR, Butcher EC. Role for CXCR6 in recruitment of activated CD8+ lymphocytes to inflamed liver. J Immunol. 2005;174(1):277–283. doi:10.4049/jimmunol.174.1.277.

99. Heydtmann M, Lalor PF, Eksteen JA, Hubscher SG, Briskin M, Adams DH. CXC chemokine ligand 16 promotes integrin-mediated adhesion of liver-infiltrating lymphocytes to cholangiocytes and hepatocytes within the inflamed human liver. J Immunol. 2005;174(2):1055–1062. doi:10.4049/jimmunol.174.2.1055.

100. Cendon C, Du W, Durek P, Liu YC, Alexander T, Serene L, Yang X, Gasparoni G, Salhab A, Nordström K, et al. Resident memory CD4 + T lymphocytes mobilize from bone marrow to contribute to a systemic secondary immune reaction. Eur J Immunol. 2022;52(5):737–752. doi:10.1002/eji.202149726.

101. Kärber G. Beitrag zur kollektiven Behandlung pharmakologischer Reihenversuche. Naunyn-Schmiedebergs Arch für Experimentelle Pathol und Pharmakol. 1931;162(4):480–483. doi:10.1007/bf01863914.

102. Zhuang Z, Lai X, Sun J, Chen Z, Zhang Z, Dai J, Liu D, Li Y, Li F, Wang Y, et al. Mapping and role of T cell response in SARS-CoV-2–infected mice. J Exp Med. 2021;218(4):218. doi:10.1084/jem.20202187.

103. Reuter D, Sparwasser T, Hunig T, Schneider-Schaulies J, Wang T. Foxp3+ regulatory T cells control persistence of viral CNS infection. PLOS ONE. 2012;7(3):e33989. doi:10.1371/journal.pone.0033989.